Report Title: Enhancement of Equilibriumshift in Dehydrogenation Reactions Using a Novel Membrane Reactor

Report Type: FINAL | Reporting Period Start Date:09/30/1996 End Date: 09/29/2000

Principal Author(s): Shamsuddin Ilias, Ph.d., P.E.
Franklin G. King, D.Sc.

Report Issue Date: 02/13/2001 DOE Award No.: DE- FG22 - 96PC96222

Submitting Organization(s)
Name & Address
North Carolina A&T State University
Department of Chemical Engineering
Greensboro, NC 27411
E-mail: ilias@ncat.edu
Tel: (336) 334-7564 Fax: (336) 334-7904

ABSTRACT

With the advances in new inorganic materials and processing techniques, there has been renewed interest in exploiting the benefits of membranes in many industrial applications. Inorganic and composite membranes are being considered as potential candidates for use in membrane-reactor configuration for effectively increasing reaction rate, selectivity and yield of equilibrium limited reactions. To investigate the usefulness of a palladium-ceramic composite membrane in a membrane reactor-separator configuration, we investigated the dehydrogenation of cyclohexane by equilibrium shift. A two-dimensional pseudo-homogeneous reactor model was developed to study the dehydrogenation of cyclohexane by equilibrium shift in a tubular membrane reactor. Radial diffusion was considered to account for the concentration gradient in the radial direction due to permeation through the membrane. For a dehydrogenation reaction, the feed stream to the reaction side contained cyclohexane and argon, while the separation side used argon as the sweep gas. Equilibrium conversion for dehydrogenation of cyclohexane is 18.7%. The present study showed that 100% conversion could be achieved by equilibrium shift using Pd-ceramic membrane reactor. For a feed containing cyclohexane and argon of 1.64×10^{-6} and 1.0×10^{-3} mol/s, over 98% conversion could be readily achieved.

The dehydrogenation of cyclohexane was also experimentally investigated in a palladium-ceramic membrane reactor. The Pd-ceramic membrane was fabricated by electroless deposition of palladium on ceramic substrate. The performance of Pd-ceramic membrane was compared with a commercially available hydrogen-selective ceramic membrane. From limited experimental data it was observed that by appropriate choice of feed flow rate and sweep gas rate, the conversion of cyclohexane to benzene and hydrogen can increased to 56% at atmospheric pressure and 200°C in a Pd-ceramic membrane reactor. In the commercial ceramic membrane reactor the observed conversion was about 38% under similar conditions. These conversions are significantly well over the equilibrium conversion of 18.7% in a conventional reactor. Thus, by selective removal of hydrogen in Pd membrane reactor it is now possible to shift the thermodynamic equilibrium to the right to increase the yields of equilibrium limited reactions.

In developing Pd-ceramic membranes, eight porous ceramic and stainless steel substrates were investigated to find the influence of the substrates to the morphology of the Pd membranes plated on them. The results indicated that the pore size and coarseness of the substrate are the most important factors when choosing the right substrate for good Pd membrane plating. A modified electroless plating procedure had been developed for stainless steel substrate. The membrane plated by this method is much better than the conventional one. But it still needs improvement to make a defect free Pd membrane.

TABLE OF CONTENTS

LIST OF TABLES

LIST OF FIGURES

EXECUTIVE SUMMARY

To demonstrate the usefulness of our Pd-ceramic composite membranes in membrane-reactor configuration, we studied the dehydrogenation of cyclohexane using planar Pd-ceramic discs. The reactor was packed with Pt-catalyst pellets. The Pd-ceramic membrane discs were fabricated by electroless deposition method. The experimental results suggest that by using our new membrane in membrane reactor, we can achieve a conversion of over 55% against the equilibrium conversion of 18.7% under identical operating conditions. Thus, it possible to shift the equilibrium significantly to the right by recovering hydrogen simultaneously as permeate product from the reactor using of H2-selective Pd-ceramic membrane.

INTRODUCTION

INTRODUCTION

Membrane reactors are unique in that they are capable of combining chemical reaction and separation in a single-unit operation. The membrane, being selective to one or more of the product or reactant species, can be used to improve the yields of thermodynamically limited reactions.

Low-temperature applications were the first to benefit from this concept. Most of them utilize organic membranes. The availability of high-temperature, porous, ceramic and metallic membranes has opened up new avenues to researchers and engineers for carrying out catalytic processes at elevated temperatures. Ceramic and metallic membranes can function for prolonged periods at high temperatures with great stability, possess improved pore size controllability and have higher rates of heat transfer. The development has renewed interest in the use of high-temperature catalytic membrane reactors and is the subject of recent reviews [1,2].

One particular class of reactions of industrial importance is the dehydrogenation of lower alkanes. These yield valuable commodity chemicals for the production of alcohols, gasoline blends and polymers. However, these reactions are also limited by their thermodynamic equilibrium and to obtain higher yields, very high temperatures are required resulting in losses in both selectivity and overall catalyst activity. An incentive therefore exists for a process that has the capability of overcoming the thermodynamic equilibrium while maintaining the integrity of the catalyst and improving the product yield. Membrane reactor technology appears to be promising since the selective removal of hydrogen from the reaction products would inevitably tend to shift the equilibrium towards increased product yield. The integration of chemical reaction and separation in a membrane reactor would then result in better rate control because of shorter contact time and reduced temperature of operation.

Experimental investigations have been attempted for reactions accompanying membrane separation with the objective of shifting the equilibrium towards increased conversion [3,4,5]. However, computer simulations and experiments have established that there is a limitation on the performance of microporous membrane reactors and it is almost impossible to make the reaction proceed beyond a certain level of conversion without the need to recycle the unreacted feed since some feed also passes through the micropores of the membranes into the separation side [6,7].

This limitation can be overcome by using a membrane that is selective only to products. Palladium and palladium alloys are the current preferred methods for removing hydrogen exclusively. However, existing commercially available palladium membranes are too thick to provide economic rates of permeation and palladium being an expensive metal, a great thickness also means more cost. Although the selectivity of microporous membranes is limited, they could be employed as substrates in which a thin metal layer of a dense membrane material such as palladium may be deposited to form a coherent layer having exclusive permeation to hydrogen.

RESEARCH OBJECTIVES

The overall objective of this project is to develop inorganic and composite membranes for in-situ separation of hydrogen and equilibrium shift in catalytic membrane reactors. The specific objectives of this research are to:

1. Design and fabrication of catalytic membrane reactor using thin film palladium-composite membrane for dehydrogenation of cyclohexane to benzene
2. Conduct dehydrogenation reaction experiments to study the equilibrium shifts and hydrogen permeation characteristics
3. Develop a theoretical foundation for equilibrium shifts and hydrogen transport in the membrane reactor

This report summarizes the performed under DOE Grant No. DE-FG22-96PC96222, covering the period 09/01/1996 to 08/31/2000.

EXPERIMENTAL METHODS

To develop a new class of HZ-selective inorganic membrane, in our lab we have used electroless plating to deposit a palladium thin-film on microporous ceramic substrate [8,9]. Electroless plating is a controlled autocatalytic deposition of a continuous film on the surface of a substrate by the interaction of a metal salt and a chemical reducing agent. In this work, to compare the influence of the different substrates on the structure of palladium membranes, eight different of microporous substrates were tested. The source, pore size and material construction of the substrates are given in Table 1.

Table 1. Information about different substrates used

No.	Pore size	Material	Company
1	0.2 micron disc	Alumina	Coors Technical Ceramics Co.
2	0.5 micron disc	Alumina	Koch Membrane System, Inc
3	0.15 micron disc	Alumina	Velterop BV (Netherlands)
4	0.2 micron tube*	Alumina	OSMONICS
5	0.2 micron tube*	Alumina	USFilter
6	0.5 micron disc"	Stainless steel	Mott Corporation
7	0.2 micron tube*	Stainless steel	Mott Corporation
8	0.5 micron tube*	Stainless steel	Mott Corporation

Pore size of the inner side of tube.

Made from 8.5" X 10" X 0.6", 0.5 um, 316L SS porous sheet

ELECTROLESS PLATING

Electroless plating is a three step process, which include substrate cleaning, sensitization and activation, and electroless plating. The basic principles of electroless plating are well established and may be found elsewhere [8,9]. For brevity, details are not repeated here.

Because of the material difference, the electroless plating of stainless steel is slightly different from ceramic. The major difference is in the cleaning step. Ceramic substrate can be easily cleaned by acid and alkali solution while stainless steel substrate had to be cleaned by organic solvent.

Substrate Cleaning: The ceramic substrates were cleaned by boiling in 0.1N NaOH solution for 10 minutes, followed by 10 minutes boiling in O.1N HCL solution. The substrates were then washed in boiling distilled water for 10 minutes, and then dried at 120 °C overnight. The cleaning was done to remove any organisms, residual metals and dust. The cleaning step is vital to ensure that activation and plating take place across the exposed surface and into the pores of the substrate.

Sensitization and Activation: The compositions for sensitization and activation solution are list in Table 2. For discs, one face and the edges were wrapped with Teflon tape to prevent sensitization and activation. For tubes, the outer sides of the tubes were wrapped with Teflon tapes. They were dipped successively in acidic SnC12 solution followed by acidic PdC12 solution at room temperature. Each dip lasted for about 4 to 5 minutes and was followed by washing with distilled water for about one minute between each dip. They were dipped in the SnC12 and PdC12 solutions alternately for several times to ensure sensitization and activation of the substrate for electroless plating.

Table 2. Composition of sensitization and activation solutions

Sensitization solution		Activation Solution	
Component	Concentration	Component	Concentration
SnC12-21-120	1.19g/1	PdC12	0.09g/1
HC1	0.2N	HCl	0.2N

Electroless plating: The activated discs and tubes were wrapped with fresh tape, and then put in the electroless plating solution for an hour. The plating step was continued until a dense membrane was made. Each time the substrate was dipped into the fresh plating solution. Then they were dried in oven at 80 °C for 1 hour.

The recipe used for electroless plating is given in Table 3. This recipe is somewhat different from what was used in our lab by former students [8,9]. At the beginning of this work, we used the recipe of the former students and observed that the electroless plating solution becomes unstable in 2 to 3 hours after hydrazine is added. We improved the plating solution by applying the research result of Yeung [10]. They reported that high concentration of NH40H keeps the bath stable while low NH40H concentration has high initial deposition rate but quickly

leads to bath decomposition and bulk precipitation of Pd metal. In earlier plating solutions we used 390 ml/l 5N ammonium hydroxide solution. Currently we are using 600 ml/1 29.5 wt% solution. The amount chosen now is a compromise between the deposition rate and stability of the plating solution. With increased amount and concentration of NH40H, the plating solution can stay stable for at least 24 hours for the same amount of hydrazine was added. As a result, adding additional hydrazine to the plating solution we can now reduce more Pd from the same solution. Because of the high price of PdC12, this certainly is a very good way to make plating solution more efficient.

Table 3. Electroless plating bath composition

Component	Concentration
Palladium chloride	5.4 g/1
Ammonium Hydroxide (29.5% wt)	600m1/l
EDTA	40g/l
Hydrazine (1 molar solution)	IOml/1
PH	l 0.8
Temperature	Room temperature

ELECTROLESS PLATING OF STAINLESS STEEL SUBSTRATES

The electorless plating process for stainless steel substrates is very much similar to that of ceramic substrate with the only difference in cleaning step. Porous stainless steel substrates were cleaned in an ultrasonic water bath using hot distilled water. The substrates were in the ultrasonic bath for about an hour and then dried in an oven at 120 °C for one hour. After drying, the substrate was dipped in carbon tetrachloride solution in an ultrasound bath and cleaned for about an hour. It was then dried in an oven at 120 °C for an hour. The cleaning process was repeated again to ensure good cleaning of the substrate for subsequent plating steps.

After plating stainless steel discs, we found from the EDX results that palladium is more difficult to be plated on stainless steel substrate than on alumina substrate. The difficulty in plating may be linked to inadequate cleaning of the substrate. This could be a serious issue, particularly for tubular substrate because of its geometry. To get a better understanding on

cleaning of stainless steel substrate, we consulted Mott Corporation, who provides us the substrate. Per suggestion from Mott, we contacted Carolina Filters (South Carolina) because of their experience in porous metal cleaning. Using Carolina Filters' suggestion, we cleaned the porous stainless steel tubes by bubbling air through the tube in ultrasonic bath using a commercial cleaning. One end of the tube was connected to an air line with on/off valve to bubble air through the tube. The tube was immersed in boiled water for 10 minutes, after that the tube was dipped in commercial cleaner Alconox solution (1% solution) in the ultrasonic bath. Air was blown in the tube for about 30 seconds then off for 2 minutes, it kept on and off during the cleaning procedure to help the fluid wash through the pores. The cyclic operation was repeated several times. Then the tube was immersed in distilled water in the ultrasonic bath to wash off the detergent while connected to the air line. The whole cleaning process was repeated twice to ensure cleaning.

In the electroless plating process, for stainless steel tubes we doubled the concentrations of PdC12 and SnC12 for the sensitization and activation steps because of our suspicion that the original concentration might not be enough for stainless steel.

SEM AND EDX RESULTS OF PD-MEMBRANES ON CERAMIC & STAINLESS STEEL SUBSTRATES

The substrates and Pd-membrane films were analyzed by SEM and EDX in the Mechanical Engineering Department of NCA&TSU. SEM (Scanning Electron Microscopy) shows the morphology of membrane. EDX (Energy Dispersive X-ray analysis) reveals the elemental composition of the surface or film.

Figure 1 to Figure 7 show the SEM results of the Pd membranes plated on different materials. In each figure, there are the pictures for the substrate before plating and after plating. For the 0.5-micron stainless steel disk and tube, only one set of picture is shown. No SEM ¡mages of the US Filter's 0.2-micron ceramic tube were taken because the tube must be broken before taking the SEM for the inner side of the tube. The tube cannot be used anymore if the picture is taken. The ceramic tubes are over a hundred dollar apiece and economic considerations dictated us not to resort destructive exercise for SEM image of the substrate. The EDX result for Pd membrane plated on 0.15-micron ceramic disk from Velterop is shown in Figure 8.

The influence of the substrate's structure on the Pd membrane plated on it is clearly shown in Figure 1 to Figure 7. The surface morphology of Pd membrane is the reflection of the

structure of the substrate. The comparison of the ceramic substrates indicates that the smaller the pore size of the substrate, the denser the Pd membrane. While comparing the substrates with the same pore size, the ceramic substrates from Coors (Figure 1) and OSMONICS (Figure 4) with 0.2 micron, it shows the influence of the coarseness of the substrate on the plated membrane. Although, both substrates have nominal pore size of 0.2 micron, we found that the substrate from OSMONICS is more uniform than the Coors' substrate in physical appearance. Uniform and dense Pd-film on OSMONICS' substrate is attributed to its surface uniformity.

When comparing ceramic and stainless steel with the same pore size, the Pd-membranes plated on ceramic substrate has fewer pinholes and is more uniform than the ones plated on stainless steel. The results of the SEM clearly show the role of substrate surface morphology on the final Pd-film quality. Both the pore size and the coarseness of the substrate must be considered. When it is possible, always use the substrate with smallest pore size and finest structure.

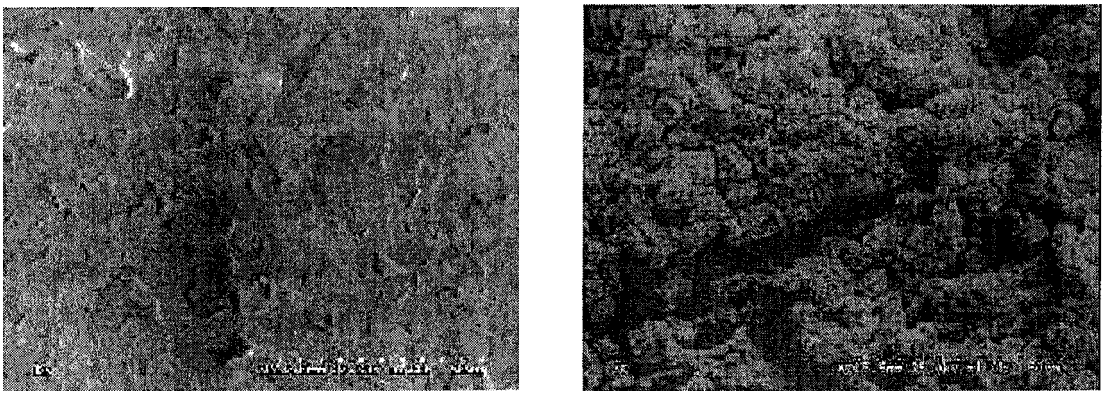

(a) (b)

Figure 1. SEM Micrograph of (a) 0.2 micron pore size ceramic substrate from Coors (b) Pd film deposited on the substrate

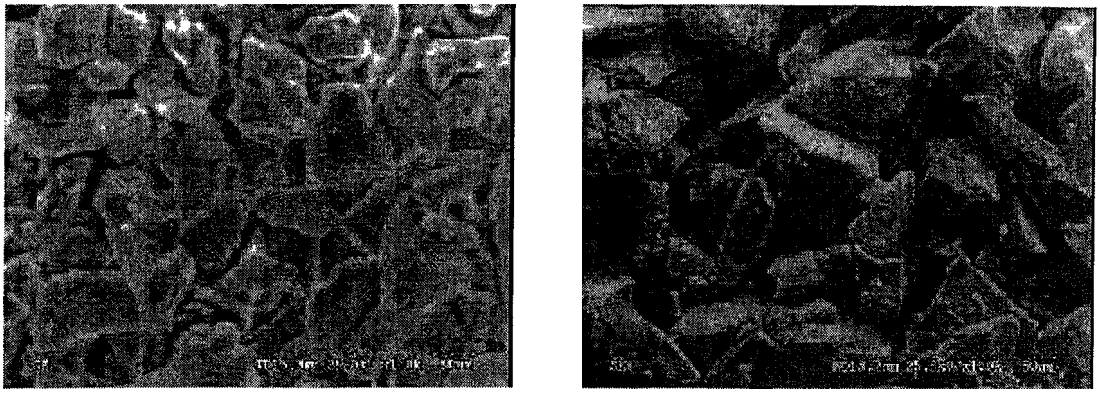

(a) (b)

Figure 2. SEM Micrograph of (a) 0.5 micron pore size ceramic substrate from Koch (b) Pd film deposited on the substrate

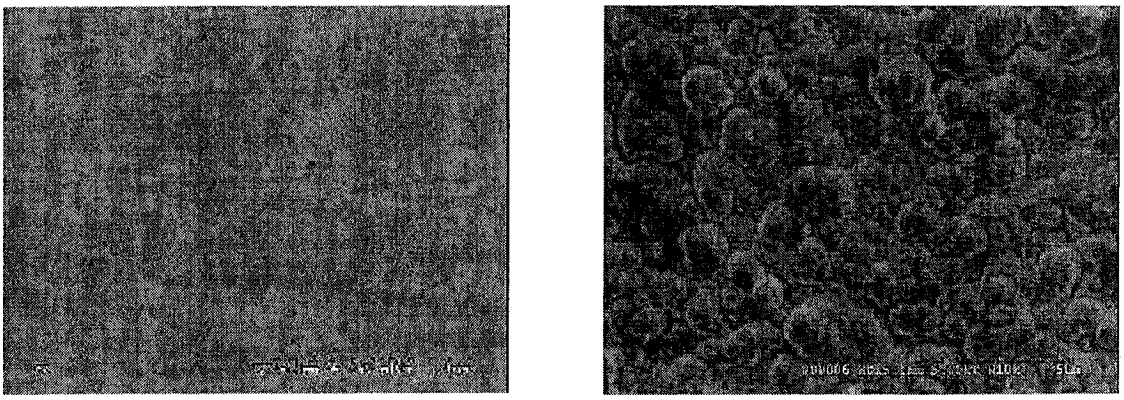

(a) (b)

Figure 3. SEM Micrograph of (a) 0.15 micron pore size ceramic substrate from Velterop (b) Pd film deposited on the substrate

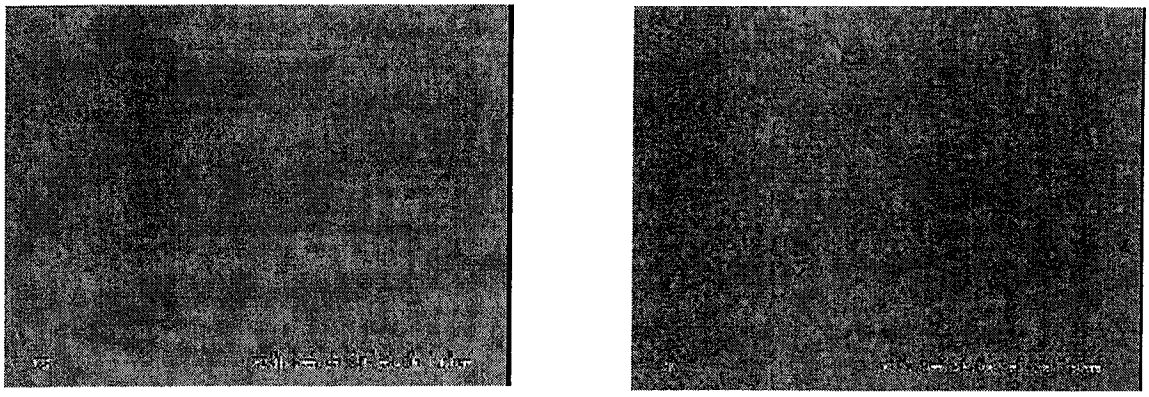

(a) (b)

Figure 4. SEM Micrograph of (a) 0.2 micron pore size ceramic tube from OSMONICS (b) Pd film deposited on the inner side of the tube

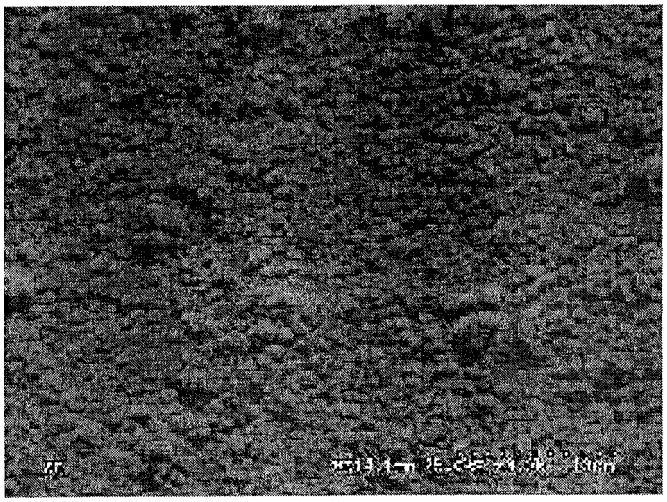

Figure 5. SEM Micrograph of Pd film deposited on the inner side of the tube from USFilter with 0.2 micron pore size

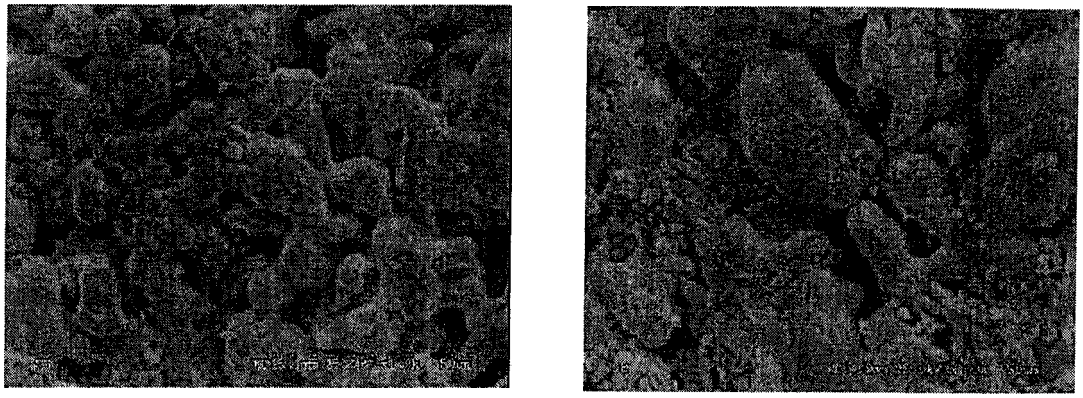

(a) (b)

Figure 6. SEM Micrograph of (a) 0.5 micron pore size stainless steel substrate from Mott (b) Pd film deposited on the substrate

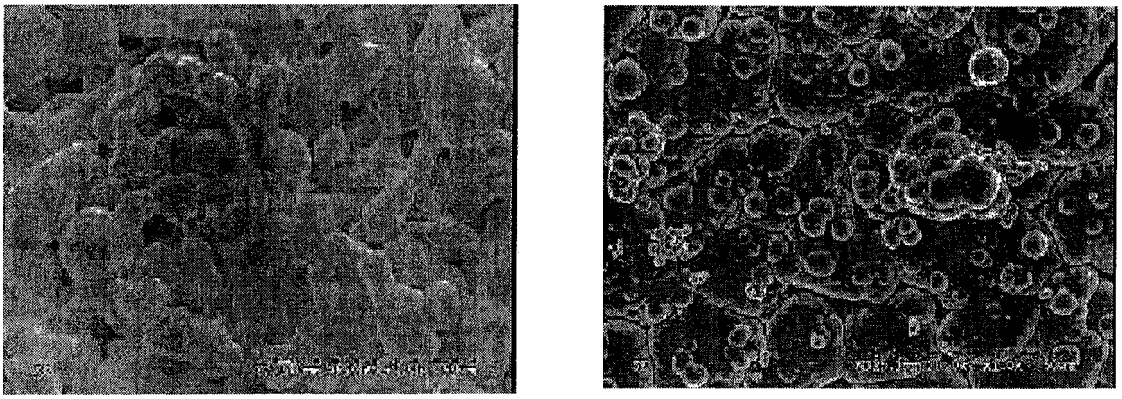

(a) (b)

Figure 7. SEM Micrograph of (a) 0.2 micron pore size stainless steel substrate from Mott (b) Pd film deposited on the substrate

Spectrum label: EDX for Pd membrane on ceramic from Velterop

Elmt	Spect. Type	Element	Atomic
Al K	ED	**0.47**	1.81
SiK	ED	0.23	0.84
Ar K	ED	0.45*	1.17*
Pd L	ED	**98.85**	96.19
Total		**100.00**	100.00

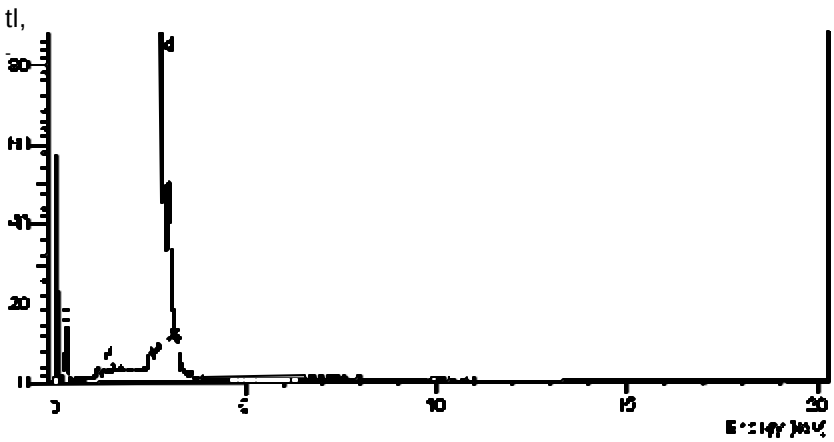

Figure 8. An example of the EDX result for Pd membrane on ceramic disk from Vel.terop

MODIFIED ELECTROLESS **PLATING** PROCEDURE

One 13-inch long, 0.2 micron, stainless steel tube was cut **into** three pieces. Two **pieces** were about six inches long and one about one inch long. One of the six inch long tube and the one inch long tube were plated together with the traditional electroless plating **method** as stated in the previous section. The SEM ii-nage of the small piece tube was shown in Figure 3.7.

Because of the **sai-ne** condition, we **assumed that** the long tube has the similar surface morphology as the short one. We did not take the SEM image of the long tube because if the tube is cut to take a sample for the SEM, the ends of the tube become porous and cannot be used for the permeability study. From the SEM pictures, we can see **that there** are still **soi-ne** pinholes even the tube was plated nine times. The leak test showed that the tube could not even hold the

pressure for ten seconds. It seems that palladium atoms are not as attached to stainless steel as they are attached to ceramic substrate. We found that the traditional plating method was not good enough for stainless steel substrate.

A modified electroless plating method then was used. It used osmotic pressure as the driving force to make the solvent of the plating solution get into the tiny holes (pores) of the substrate to help plate palladium onto the wall of the holes, then block them with the growth of the palladium film. Secondly, osmotic pressure would press palladium onto the substrate to make the membrane compact and robust.

Because different solutions have different osmotic pressures, the net osmotic pressure difference of two solutions can be the driving force to make the solvent of the solution, which has lower osmotic pressure flow to the solution with higher osmotic pressure. So if we find a solution, which has higher osmotic pressure than the electroless plating solution, the solvent of the plating solution will be driven pass through the barrier, in this case it is the stainless steel tube, to the other solution.

There are a large number of chemical solutions, which have high osmotic pressures. For example, a 3.5 molal CaC12 aqueous solution has an osmotic pressure of about 517 bar at room temperature, while similar concentrations of NaCl, KCI, and sucrose exert about 200,160 and 100 bar, respectively [11]. We chose sucrose as the solution of higher osmotic pressure than the plating solution in our experiment. We did not use chloride solutions of higher osmotic pressure in the electroless plating process for cross-contamination problem. In our future work, we plan to co-deposit Pd-Ag by electroless deposition, using silver nitrate (AgN03) for the silver deposition. For this reason, we do not want the CI ions to interact with Ag ions to make AgCI precipitation and deactivate the silver deposition.

We can reach high enough osmotic pressure by raising the concentration and the temperature of the sucrose solution because osmotic pressure is a function of concentration and temperature. Normally, osmotic pressure increases with increasing concentration and temperature. There are different theories for calculating osmotic pressure. The osmotic pressure is related to temperature and concentration by the Van't Hoff equation [12] as:

$$IIV = RT \qquad (1)$$

or

$$II = RTC \qquad (2)$$

where V is the molar volume of the solution, C is the concentration of the solution, R is taken as being equal to the gas constant and T is the absolute temperature.

It has been shown by experimental measurement of osmotic pressure that the Van't Hoff equation is applicable only for very dilute solution. As the concentration increases the deviations become more and more marked, the observed osmotic pressure being greater than the calculated values. Better agreement with experimental data is obtained by using a modified equation proposed by H.N. Morse [12] in which V, the volume of the solution is replaced by V', the volume of the solvent associated with 1 mole of solute. Thus,

$$\Pi V' = R T$$

For dilute solution with multiple solutes, the osmotic pressure may be obtained from the following equation [13]:

$$\Pi Z - - \frac{RT}{V_{m}} \ln x \qquad (4)$$

or

$$\Pi - \frac{RT}{V_{m}} \qquad (5)$$

where V_m is the molar volume of the pure solvent, $\sum x_j$ is sum of the mole fractions of the various solutes, and x is molar fraction of solvent.

Equation (4) is derived from the chemical potential equilibrium of an osmotic system consisting of pure solvent together with a solution and an intervening membrane, which is permeable to the solvent. This is applicable to ideal solution. Equation (5) is a simplification of Eqn. (4), noting that $x = 1 - Y$, x_j, and when $\sum x_j$ are very small, we have $\ln x = -\sum x_j$. Although these equations can be used to predict the osmotic pressure of the solutions, because of the limitations of these equations, the calculated osmotic pressure is lower than the experimental data [12].

Even though there is observed osmotic pressure available for sucrose, we cannot get the experimental data for the electroless plating solution. We choose to calculate the osmotic pressures of the two solutions by equations derived from same origin to minimize the error. For example, the experimental osmotic pressure for 6 molal sucrose solution at 60 °C is about 248 atm, while the computed osmotic pressure from Eqn. (3) is 164 atm. Under similar conditions, if we use Eqns. (4) and (5), we find the osmotic pressures for plating solution as 156 and 148 atm,

respectively. The difference in the measured and computed osmotic pressures of the sucrose solution is significant. However, for the plating solution, the difference in the osmotic pressure estimates is not that great. To be on the conservative side, we used 164 atm as the osmotic pressure of sucrose and 156 atm for the plating solution.

Although the difference of the calculated osmotic pressures of the two solutions is not very big, about 8 atm at 60 °C, this is still a high pressure that is not easily obtained by other means. The modified electroless plating process is shown schematically in Figure 9. The plating equipment includes a pump, the plating solution and a water bath. Tygon tubing (1/4 in ID x 3/8 in OD) from Fisher Scientific was used to connect the pump, plating solution and the stainless steel tube. Then the stainless steel tube was immersed in the sucrose solution, which was in the heated water bath maintained at 60 °C. The plating solution was circulated through the stainless steel tube using the pump, the flow rate was kept constant at 60 ml/min. The plating solution was not heated otherwise it would be decomposed after 30 minutes of heating.

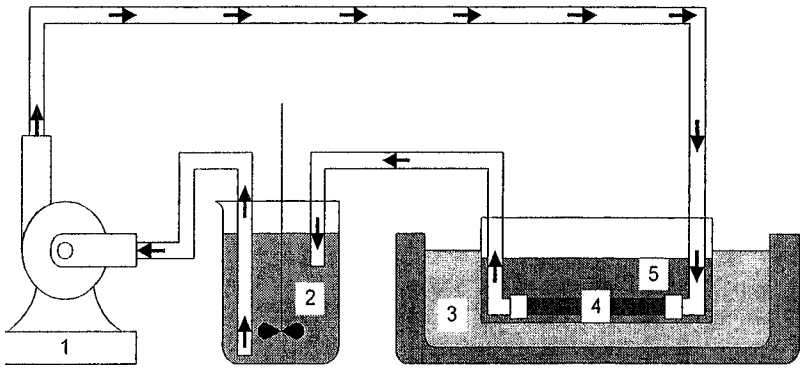

1-Pump
2 - Plating solution
3 - water bath
4 - stainless steel or ceramic tube
5 - sucrose solution

Figure 9. Modified electroless plating procedure

Since the plating solution is cycled in the loop (Figure 9), one would expect a much lower temperature of plating solution (much less then 60 °C). As a result, we would expect much higher osmotic pressure difference between the sucrose and plating solution, which is definitely larger than estimated 8 atm pressure. We decided to try the 6 molal sucrose (6 mole of solute in

1000 gram of solvent) solution to see if the osmotic pressure is enough to plate a dense palladium film on the stainless steel substrate.

Before plating, the pump and tubing were rinsed three times with deionized water by circulating it through the loop. Then water was substituted by plating solution in the container, the pump operated at its maximum flow rate to mix the plating solution with the rinse water, which is left in the pump, and tubing. After ten minutes, the solution was considered uniform; the flow rate was then reduced to 60 ml/min.

After plating, deoinized water was again circulated in the loop twice to clean the pump and tubing, making sure that no plating solution was left in the loop. Otherwise the pump and tubing would be plated with palladium. At the beginning of the plating, the plating solution passing through the inside of the tube can be seen coming out to the sucrose solution. The streams were moving upwards. This proved the help of osmosis. Because of losing the plating solution to the sucrose solution, the plating solution and the sucrose solution were changed every one hour with fresh solutions to maintain the osmotic pressure difference. After three times, the streams were seldom seen. So the fourth bath was kept for a long time, about 6 hours. After two more runs of plating like this, the tube was cleaned with deionized water thoroughly and then dried in air.

The Pd-plated stainless steel tube was tested for leaks and pinholes at room temperature with argon. In the leak tests, we found at pressure of 20 psi, the pressure drop is about 0.2 to 0.3 psi for ten minutes, which is in the allowable range for dense, pinhole free membrane. Next, the tube was heat treated at 723K under argon atmosphere to avoid hydrogen embitterment. Then the membrane tube was tested for perm-selectivity using a hydrogen and methane mixture at 473K. During the permeability test, we observed that the pressure was dropping suspiciously fast, so the test was ended to find out if the Pd membrane had deformed. Argon was applied again for leak test, this time, the pressure dropped very fast, about 0.1 psi per minute. It means the Pd membrane had deformed by the adsorption and desorption of hydrogen as stated in Chapter 2. So the osmotic pressure we used is not high enough to make the membrane compact as the way to resist the deformation caused by hydrogen adsorption and desorption. A solution with much higher osmotic pressure must be found to fulfill this function.

MODELING OF MEMBRANE REACTOR

In this study, we considered - a tubular membrane reactor for the dehydrogenation reaction. Pt-A1203 catalyst pellets are loaded inside the palladium-ceramic tube. Hydrogen produced by the reaction permeates through the membrane into the shell side. Argon is used as the carrier gas in the feed side and as sweep gas in the shell side to remove permeated hydrogen. Concentration of hydrogen near the membrane wall is depleted due to permeation. As a result, a concentration gradient is developed in the radial direction. A two-dimensional pseudo-homogeneous model was developed to describe the transport mechanism through the catalyst bed. In this paper, we present our modeling work.

MODEL FOR DEHYDROGENATION OF CYCLOHEXANE IN A MEMBRANE REACTOR

In order to develop a model for a membrane reactor, one needs to consider the reaction kinetics and the transport mechanisms through the membrane as well as through the catalyst bed. In the present work, a palladium-ceramic membrane reactor is studied numerically for the dehydrogenation of cyclohexane to benzene and hydrogen. Pt/A1203 catalyst pellets are assumed inside the membrane tube, i.e. reaction side. The dehydrogenation of cyclohexane on supported Pt/A1203 catalyst is a reversible reaction, which can be expressed as:

$$C_6H_{12} \rightleftharpoons C_6H_6 + 3H_2 \quad \text{or symbolically} \quad C \rightleftharpoons B + 3H \tag{6}$$

A number of rate expressions have appeared in the literature to describe the dehydrogenation of cyclohexane to benzene and hydrogen. Published expressions vary from empirical expressions that are more practical to ones based on fundamentals. In Table 4, a summary of rate expressions is given that are pertinent to this work [14-16]. In all cases, the dehydrogenation reaction is considered to be catalytic and Pt/A1203 is used as the catalyst.

The rate expression used by Itoh [16] is essentially based on some minor modifications of the Langmuir-Hinshelwood-Hougen-Watson mechanisms. In his work, Itoh [16] used this expression in the analysis of membrane reactor using palladium. The expressions for the constants are:

$$K_B = 2.03 \times 10^{-10} \exp\left(\frac{6270}{T}\right), \text{ Pa}^{-} \tag{7}$$

$$K_p = 4.89 \times 10^{35} \exp\left(\frac{3}{T}\right) \text{ Pa}^3$$

$$k = 0.211 \exp\left(-\frac{4270}{T}\right), \text{ molhn}^3 \cdot \text{Pa} - \text{s}$$

Here K_p is the pressure equilibrium constant, K_B is the adsorption equilibrium constant of benzene, and k is rate constant.

Table 4. Rate expressions for dehydrogenation of cyclohexane proposed by different investigators

Investigators (Year)	Rate Equation	Remarks
Shinji et al. 1982 [14]	$r_B = k\left[P_C - \frac{P_H^2 P_B P_H}{K_P}\right]$	empirical Homogeneous Reaction, expression
Itoh et al. 1985 [15]	$r_C = -k_0 e^{-E/RT}\left[P_C - \frac{P_B P_H}{K_P}\right]$	Improved from the previous expression
Itoh, 1987 [16]	$r_C = -\frac{k(KPKC / PH - PB)}{I+KBKPPC}$	More realistic model, phenomena considered adsorption

TRANSPORT MECHANISM THROUGH PALLADIUM-CERAMIC MEMBRANE

The Pd-ceramic membrane is nonporous. No pore space is available for diffusion. The transport of gases through nonporous membranes occurs by a solution-diffusion mechanism. The gas molecules dissolve in the membrane surface on the high-pressure side of the membranes. The gas molecules then diffuse through the membrane phase and desorb at the low-pressure side. Different investigators have studied the mechanism of hydrogen transport through the palladium membrane [17,18] and palladium-ceramic membrane [1,9]. The hydrogen flux was given by:

$$N_H = \frac{Q_H}{t}(P_H - P_H) \qquad (10)$$

where P_H and P_H are the hydrogen partial pressures of feed side and separation side, Q_H is the permeability and t is the membrane thickness. The values of n range from 0.5 to 1. The value of 0.5 implies that the transport of hydrogen through the bulk of metal is rate determining and that equilibrium is established at the surface, i.e. an equilibrium between hydrogen molecules in gas

phase and hydrogen atoms dissolved in the metal. The hydrogen concentration is proportional to the square root of hydrogen pressure, which is known as Sievert's law [18]. The result is expressed as:

$$N_H = \frac{Q_x}{t}(P_x^{0.5} - 1^{0.5})$$

A value of n equaling 1 implies a slow, rate determining surface reaction of hydrogen with palladium. The transport of hydrogen through a Pd-ceramic membrane does not follow the Sievert's law because the value of n is different from 0.5 [9,19,20]. Thus, it is necessary to develop a generalized model for all values of n, $0.5 \leq n \leq 1$.

TWO-DIMENSIONAL PSEUDO-HOMOGENEOUS MEMBRANE REACTOR MODEL

Figure 10 shows the schematic of the membrane reactor. Pellets of Pt-A1203 catalyst are assumed inside the palladium-ceramic membrane tube. Hydrogen produced by the reaction permeates through the membrane into the shell side. Argon is used as the carrier gas in the feed side and as sweep gas in the shell side to remove the permeated hydrogen. The concentration of hydrogen near the membrane wall is depleted due to permeation. Hence a concentration gradient occurs in the radial direction. There are two types of models to describe the transport mechanism through the catalyst bed: pseudo-homogeneous and heterogeneous. Pseudo-homogeneous models do not account explicitly for the presence of catalyst, in contrast with heterogeneous models, which lead to separate conservation equations for fluid and catalyst. From the discussion of different reactor models, it can be concluded that a two-dimensional model is suitable to describe the transport mechanism through the catalyst bed.

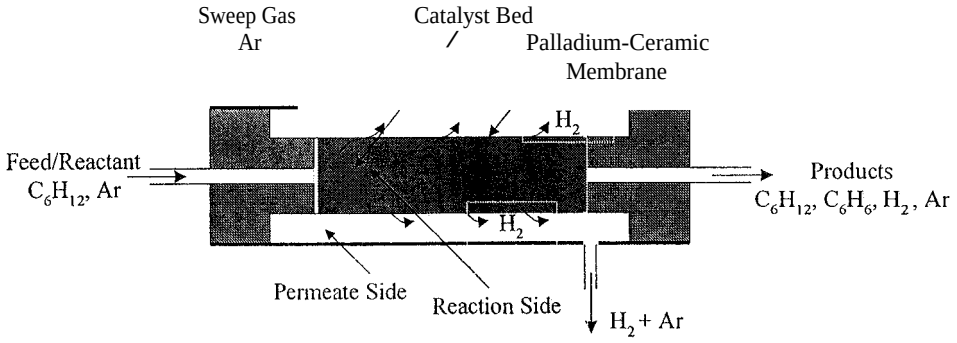

Figure 10. Pd-Ceramic Membrane Reactor

A two-dimensional heterogeneous model requires the knowledge of an effectiveness factor. For a first-order reaction it can be evaluated easily. However, dehydrogenation of cyclohexane is a complex reaction and defining the effectiveness factor is complicated. In order to avoid this complexity, a two-dimensional pseudo-homogeneous model is assumed to describe the transport mechanism through the catalyst bed. In developing the mathematical model for a membrane-reactor for the dehydrogenation reaction, the following simplifying assumptions are made:

- Isothermal, isobaric and steady-state flow through the whole reactor (both the packed-bed and separation sides) and axial diffusion is negligible.
- Plug flow is assumed through the shell side or separation side and ideal gas law is applicable
- A flat concentration profile is assumed on the separation side
- A partial pressure gradient of hydrogen in the radial direction, caused by the permeation of hydrogen through the palladium-ceramic membrane, is taken into account.
- The amount of dehydrogenation taking place on the palladium-ceramic tube is negligibly small compared to that on the catalyst pellet surface.

The permeation rate of hydrogen gas through the palladium-ceramic membrane, N_H, can be expressed by Eqn. (10), where n is different from one-half, i.e. $0.5 < n < 1.0$ [9]. Based on these assumptions, the governing equations (continuity equations) for different components in dimensionless form may be expressed as:

$$\frac{\partial (U Y_A)}{\partial Z} = -\frac{d_p l_0}{(Pe_r)_A r_1^2}\left[\frac{1}{R}\frac{\partial (D_A}{\partial R} \quad \frac{\partial^2 \quad A}{\partial R^2}\right] \tag{12}$$

$$\frac{\partial (U Y_B)}{\partial Z} = -\frac{d P l_0}{(Pe_l)_B r_l}\left(\frac{1}{R}\frac{\partial (D_B}{\partial R} \quad \frac{\partial^2 4)_B}{\partial R^2}\right) + T \tag{13}$$

$$\frac{\partial (U P C)}{\partial Z} = -\frac{d_1 l_0}{(Pe,)_c r_1^2}\left[\frac{1}{R}\frac{\partial (P C}{\partial R} + \simeq_2 (P C \quad)\right] \quad c_P \tag{14}$$

$$\frac{\partial (U Y_H)}{\partial Z} = -\frac{d P l_0}{(Pe_r)_H r_1^2}\left(\frac{1}{R}\frac{\partial (D_H}{\partial R} \quad \frac{\partial^2 (D_H}{\partial R^2}\right) + 3cp \tag{15}$$

where Z and R are the dimensional axial and radial coordinates, respectively. The component dimensionless partial pressures on the reaction and separation side are given by 4)i and y,, respectively.

The dimensionless variables are defined as:

$$1_0 = U \quad u_0 ; \quad R \quad r_1 = \frac{Ci}{R_g T} \qquad \text{with i = A, B, C, and H}$$

$$(D. = \frac{P.}{PO} = \frac{Xi}{Y- Xi} - r ; \quad (p. = \frac{Pi}{PO} = \frac{xj}{Y Xl} \frac{P;}{PO} \quad Y- (D. = 1; \quad \text{and} \quad {}_i = 1$$

where r and z are the radial and axial directions, respectively. The variables t_o is the length of the membrane reactor, r is the inner radius of membrane tube, u is the interstitial velocity of gas on reaction side, and u_o is the gas velocity at the inlet on reaction side. The pressure terms are defined as follows: P_i is the partial pressure of component i on the reaction side, P_0 is the reference pressure, p. is the partial pressure of component i on the separation side, and P_r and p are total pressures on the reaction and separation sides, respectively. The component molar flow rates on the reaction and separation sides are given by X_i and x_i respectively.

The dimensionless source term and Peclet numbers ($(Pe_r)_i$) are defined as:

$$T = \frac{R_9 T l_0 \; k(Kp(f \; P_{o(DH('B)}}{u_o P_o \quad P0 \sim H + KBKP(DC} \qquad (Per)_A = \frac{d_p}{(Der)_A}$$

$$Pe_B = \frac{u d_p}{(D_{er})_B} \cdot \quad (Per)_C - (\frac{u d_p}{uDer})_C \quad (Per)_H - \frac{u d_p}{u(Der}$$

where $(Der)_i$ is the effective radial diffusion coefficient of component i , and d_P is the sphere-equivalent diameter of catalyst pellets, and R_b is the universal gas constant.

Boundary conditions in dimensionless form are given as:

$$\text{at} \quad K=U, \; o <\_ z <\_ 1: \qquad \begin{matrix} \frac{a(DA}{ar} \_ o & \frac{a(DB}{ar} \_ o \\ \frac{a\sim DC}{ar} \_ o & \frac{aOH}{ar} = o \end{matrix} \qquad (16)$$

$$\text{at } R=I,\ 0<Z<\_1: \quad \frac{a(DA}{ar} \ r^{0} \quad \frac{a(DB}{ar} = 0 \qquad \frac{a(DC}{ar} \_O \quad \frac{a(DH}{r} = a(PH \_ pH) \tag{17}$$

where, ~3 = $\dfrac{r^{l}}{r2 - rl} \quad \dfrac{R9TQH}{PO^{1-n}\ (Der)H}$

Initial conditions in dimensionless variables on the reaction and separation sides are given by:

$$\text{at } Z=O, \quad 0 < R < 1 \qquad J(DA=(DA0 \quad (DB \quad 0 \qquad (DC = (DC^{0} \quad (DH = 0 \tag{18}$$

$$\text{at } Z=O, \quad \text{for any position} \qquad {}^{4)A}\_\_(1)^{0}{}_{0A} \qquad (DH =O \tag{19}$$

Details of the derivation of the above system of equations are reported elsewhere [12].

NUMERICAL SOLUTION

The Eqns. (12)-(15) are subject to initial and boundary conditions, Eqns. (16)-(19) can not be solved analytically. A Finite Difference method is used to solve these equations. Forward finite difference approximations for axial derivatives and central finite difference approximations for radial derivatives are used in discretization of the governing equations, Eqns. (12)-(15). The second term of the right hand side of the differential equations, except the equation for argon, is the reaction term and this is a source term. This term is highly non-linear and complex in form. It is not possible to linearlize this term. It has been treated as a constant and evaluated at a previous grid point. The source term is given as:

$$Y = (P((TB)i,J\ ,\ (YC)ij\ ,\ ((PH)iJ \_ Ti,J \tag{20}$$

The finite difference approximations of the Eqns. (10)-(13) are:

$$(U(DA)i,J+l = (U(DA)i,J + \qquad MA \quad 1 + \frac{1}{2i} \ ((DA)i+1J \_ 2((DA)i + I \_ \frac{1}{2i} \ (\Phi_A)_{i-1,j} \tag{21}$$

$$(U(DB)_{ixi+1} = (U(DB)_{i;i} + MB \left| +1i \right. ((DB)_{i+iJ-2}((DB)_{i,i} + MB \left(\left(\frac{1}{2i} \right)(4)B)_{i-jj} + Y_{iJAZ} \right. \quad (22)$$

$$(U(DC)_{i;i+1} = (U(DC_{)ixi} + MC \left(\left(\frac{1}{1} \right. + Z_j \right. (q'c)_{i+lj} - 2((\text{'}c_{)ixi} + Mc \left(\left(\frac{I}{2i} \right)((DC),\_Ij) - (pjjAZ \quad (23)$$

$$(U(1)x)_{i,i+j} = (U(fH)_{i,j} + MH_{\sim(1} + Z_j \left(OH \right)_{i+lj} - {}^{2}((DH)_{ij} + MH\, I \sim \left(\frac{I}{2i} \right. J((DH)_{i-lj} + 3T_{ijAZ} \quad (23)$$

where,

$$MA \quad \frac{d_p l_\Omega}{(Per)_A r_2} \frac{AZ}{(AR)^2}, \quad MB \quad \frac{d_p l_\Omega}{(Per)_B r_{12}} \frac{AZ}{(AR)^2}$$

$$\frac{d_p l_\Omega}{(Per)_C r_1} \frac{AZ}{(AR)^2}; \text{ and } M_H = \frac{d_p l_\Omega}{(Per)_H r_1} \frac{AZ}{(AR)^2}$$

Here M_A, M_B, M_C and M_H are dimensionless moduli including Peclet numbers for argon, benzene, cyclohexane and hydrogen, respectively. These finite difference equations are written for ith radial and jth axial grid points where AR and AZ are the radial and axial increments, respectively. They are indexed as $i = 0, 1, 2, \ldots, I (=1/AR)$ and $j = 0, 1, 2, \ldots, J (=1/AZ)$. The details of the finite difference formulation of the problem, stability analysis of the finite difference scheme and solution methodology are given elsewhere [12]. The solution algorithm used in solving is as follows:

1. Calculate Rep, Sc and Per using appropriate correlations
2. Solve the finite difference equations to determine (U(D)i,i+l
3. Assume Uj+1
4. Determine $('i,\_i+1$ from $(U(D)_{i,j+1}/Uij+1$

5. Calculate hydrogen permeation rate, $(_{NH})_{j+l}$

6. Calculate generation of moles G within the grids j and j+1

7. Compare the averaged permeation rate:

$$\{0.5\ ((NH)_j + (NH)_{j+i})\ |\ \text{with}\ \{(U_i - Uj\text{-}1 \sim * XTO + G\}$$

where XTO is the total mole flow rate at the feed inlet

8. If $\dfrac{0.5\ ((NH)_j + (NH)_{j+i}) - ((U_i - U_j\text{-}1) * XTO + G)}{(U_j - U_j\text{-}I) * XTO + G}$ <- £l, then go to the next grid j+2.

Otherwise assume new U_{j+1} and repeat steps 4-8.

SIMULATION RESULTS & DISCUSSIONS

A two-dimensional pseudo-homogenous reactor model is presented to describe the dehydrogenation of cyclohexane to benzene in a membrane-reactor. To have a better understanding of the performance of a membrane reactor, we investigated the dehydrogenation of cyclohexane in a tubular reactor. The physical parameters used in the numerical simulation are:

Reactor Dimensions:

Total reactor length,	t_0 = 0.140 m
Inner radius of inner tube,	$r_,$ = 8.50 x 10-3 m
Outer radius of inner tube,	r_2 = 8.70 x 10-3 m
Inner radius of shell,	r_3 =14.00 x 10-3 m

Dimensions of cylindrical catalyst-pellet:

Outer diameter	= 3.3 mm
Length	= 3.6 mm

Permeation parameters:

Power index,	n = 0.5
Permeability,	Q_H =1.618x $10^{-°S}$ (mol/m.Pa".s)
Permeation constant,	a =1.824 x 10-°8 (mol/s)

In numerical solutions, predicted results should be stable and also needs to be grid independent. Figure 1 I shows the effect of grid spacing on numerical solution-stability. This analysis was done for a two-component system (argon=1.348x 10-4; and

hydrogen = 7.248x 104 mol/s). From the stability analysis, the number of grid in the axial direction is N = 577 when the number of grid in the radial direction is 10. Results with N = 600 show oscillation with increasing amplitude. But for N = 700 or more, results are stable. In stability analysis, the dimensionless flow rate (U) is assumed to be unity. But the value of U decreases due to permeation of hydrogen through the membrane. As a result, larger N is required for stable operation. Variation in results obtained by setting N = 700, 800 or 900 is minimal. A value of N = 900 is about 50% more than the calculated grid numbers (577) for stability. In all work reported here, we used 50% more grids than that obtained by stability analysis.

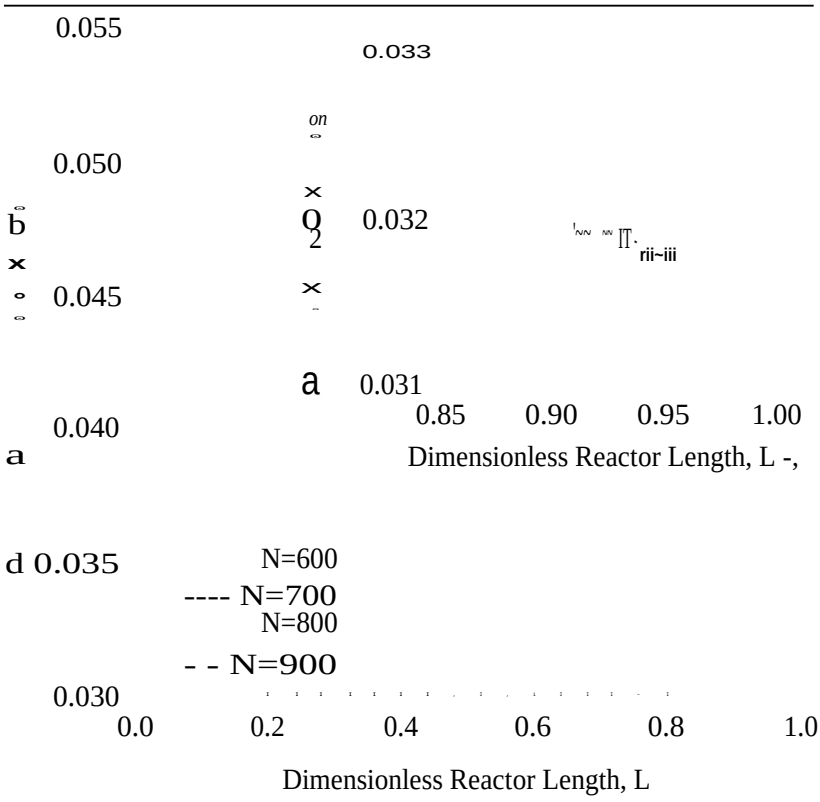

Figure 11. Effect of grid spacings on numerical stability of reactor model.

To solve the model equation for gas permeation using radial diffusion, the value for effective diffusivity in the radial direction is required. For a binary system, few data are available

and these are related to the Reynolds number(Re_p) and Schmidt number(Sc) by the following correlation [21]:

$$\frac{1}{Per} = \frac{0.4}{(Re_p Sc)^{1/2}} + \frac{0.09}{1 + \frac{10}{Re_p Sc}} \qquad \text{for } 0.4 < Re_p < 500,\ 0.77 < Sc < 12 \qquad (24)$$

No such relation is available for three or four component systems. To analyze the radial diffusion of hydrogen in four component systems, Wen and Fan's equation (Eqn. (24)) which is applicable to binary systems, is used. For non-reactive four component systems, the effect of Sc number on the dimensionless flow rate was investigated to determine an acceptable Sc number for calculation of effective radial diffusivity. The results are shown in Figures 12(a,b) and 13(a,b). It is clear from Figure 12(a,b) that the Sc numbers has no effect on the flow rate at high Reynolds number. Figure 13(a,b) reveal that the Sc number has little effect on flow rate at small Reynolds number, and essentially remains unchanged at some distance away from the inlet position.

Based on the above results, it was concluded that the effect of Schmidt number, Sc, on the numerical prediction for gas permeation is minimal. Thus, Sc =1.0 was used in the study of dehydrogenation reaction by equilibrium shift in the membrane reactor. Two sets of feed compositions were used in the analysis. Feed compositions and their corresponding dimensionless numbers are given in Table 5.

Table 5. Feed flow rate and corresponding Re_p, and Pe,-.

Feed	cyclohexane (mol/s)	Argon (molls)	Re_p	Per r
1	5.00 x 10-6	1.00x10-4	2.275	4.466
2	1.64 x 10-6	5.00 x 10^{-4}	2.010	4.098

Figures 14(a,b) show the pressure profile of benzene, cyclohexane, and hydrogen along the reactor length for Feed-2 at two sweep rates. The average pressure of cyclohexane (reactant) decreases with reactor length and the average pressure of hydrogen and benzene (products) increases. The increase in hydrogen pressure would be three times the pressure of benzene if the membrane were not used. Hydrogen pressure at the reactor outlet is less than the three times of

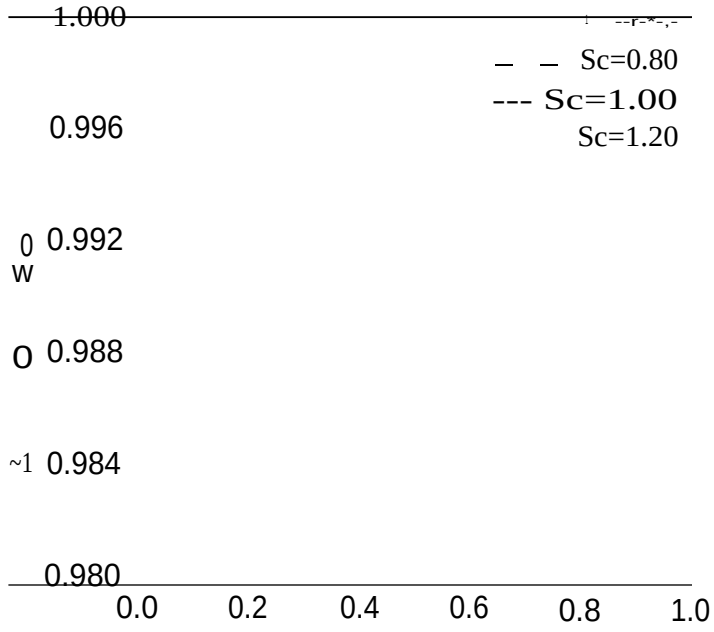

(a)

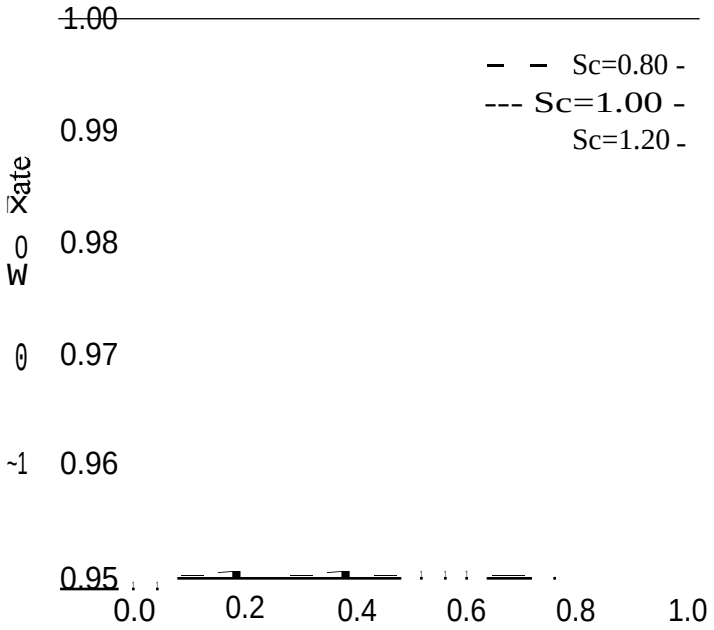

Figure 12(a,b). Effect of Schmidt number on flow rate. (a) Re p = 27.06; Sweep = 4.0E-04 mol/s; and (b) Re p = 27.06; Sweep = 1.0E-03 mol/s

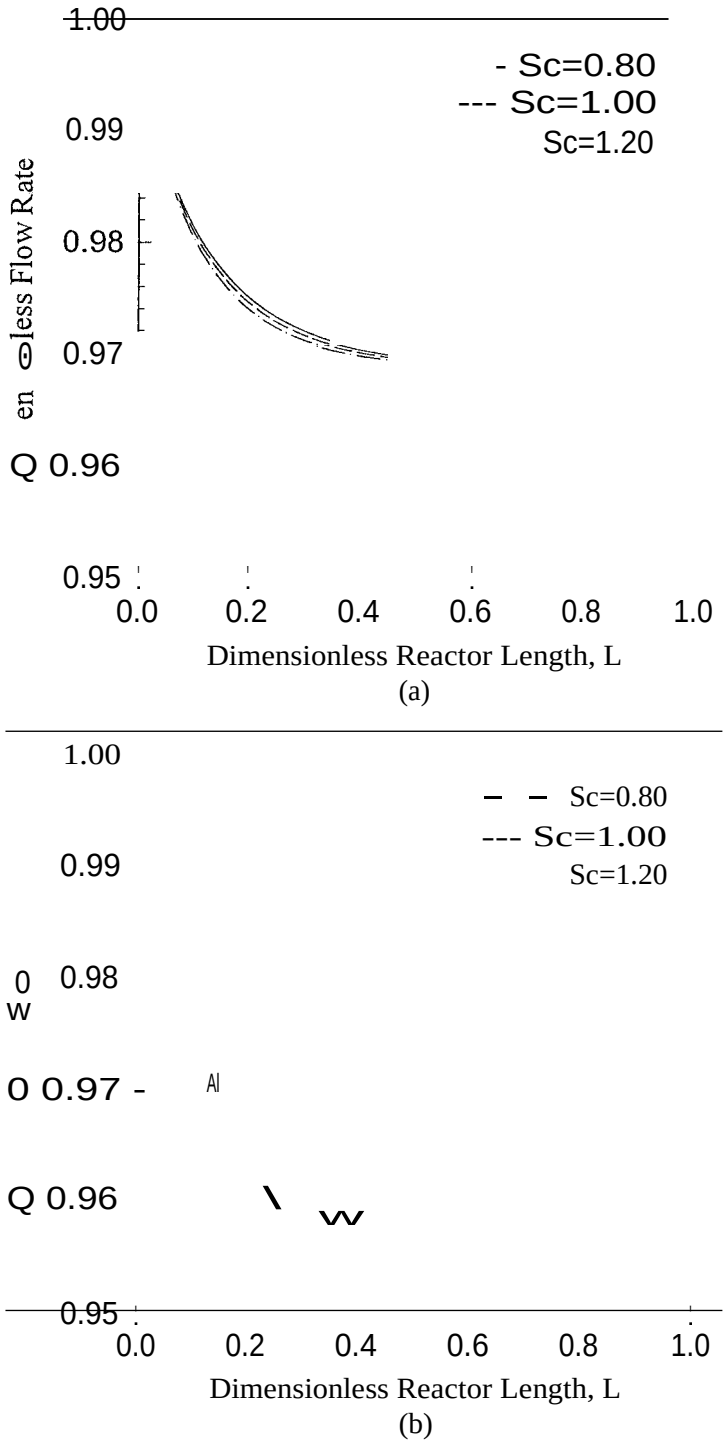

Figure 13(a,b). Effect of Schmidt number on flow rate. (a) Re_p = 2.706; Sweep =1.60E-04 mol/s; and (b) Re_p = 2.706; Sweep = 6.40E-04 cool/s.

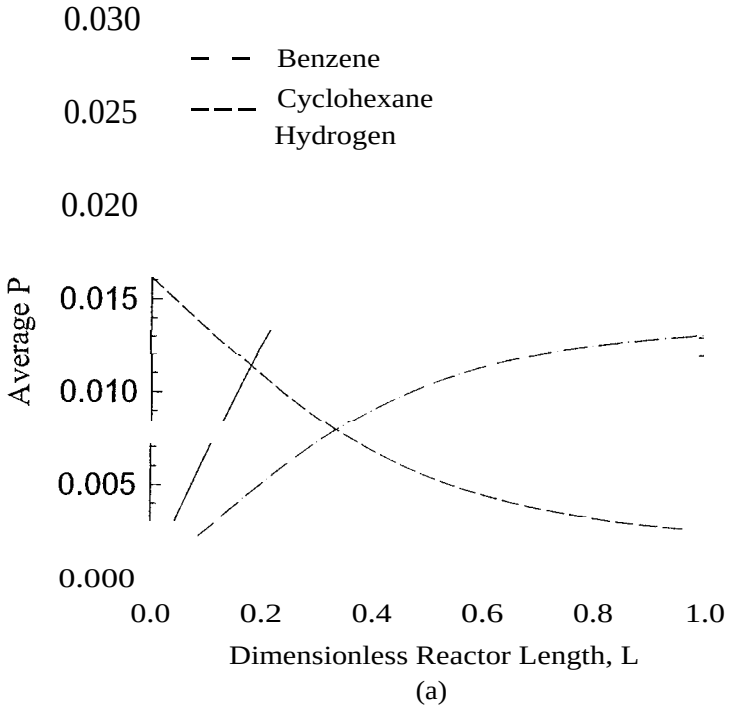

(a)

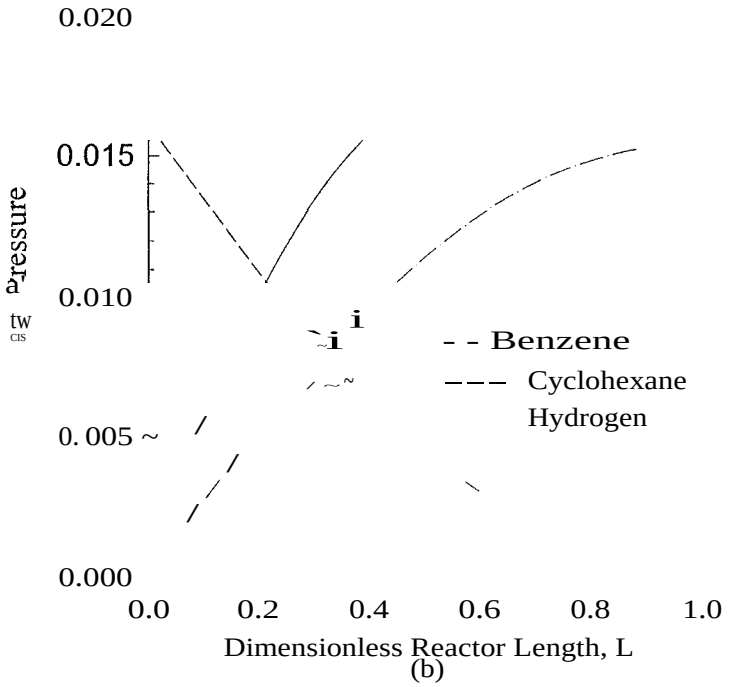

(b)

Figure 14(a,b). Pressure profile of reactive components. (a) Re_p = 2.01; Sweep = 1.0E-04 mol/s; and (b) Re_p = 2.01; Sweep = 1.0E-03 mol/s.

benzene pressure, Figure 14(a). It may be even less than the benzene pressure, when conversion is high, as shown in Figure 14(b). At high conversion of cyclohexane, one may observe a hydrogen peak. As shown in Figure 14(b), at 98% conversion a peak is observed in the hydrogen pressure profile.

Figure 15(a,b) shows a similar behavior for Feed-1. No peak in hydrogen pressure was observed, as the conversions were significantly lower. Conversions achieved are 42.6% and 48.4% at sweep rate 1.0×10^{-4} and 1.0×10^{-3} mol/s, respectively.

Figure 16 shows the %conversion of cyclohexane as a function of sweep rate for two feed compositions. At a particular sweep rate, conversion is higher for Feed-2. In Feed-2, the feed rate of cyclohexane is less. So the residence time is high for lower feed flow rate, thus giving higher conversion. For each case, conversion increases with increasing sweep rate. More of hydrogen permeates with higher sweep rates. As a result, the reaction is moving into the forward direction and giving the higher conversion by equilibrium shift.

CONCLUSIONS

A mathematical model is presented to describe the dehydrogenation of cyclohexane to benzene and hydrogen in a membrane-reactor. The model considers the radial diffusion due to selective permeation of hydrogen through the membrane wall. The concentration of the permeable component, hydrogen, near the membrane wall is depleted due to permeation. Hence, consideration of radial diffusion is required in the modeling of a membrane reactor. Equilibrium conversion for dehydrogenation of cyclohexane is 18.7%. The present study shows that 100% conversion can be achieved by the proper selection of parameters. For a feed containing cyclohexane and argon of 1.64×10^{-6} mol/s and 1.0×10^{-3} mol/s, respectively, 98% conversion is possible.

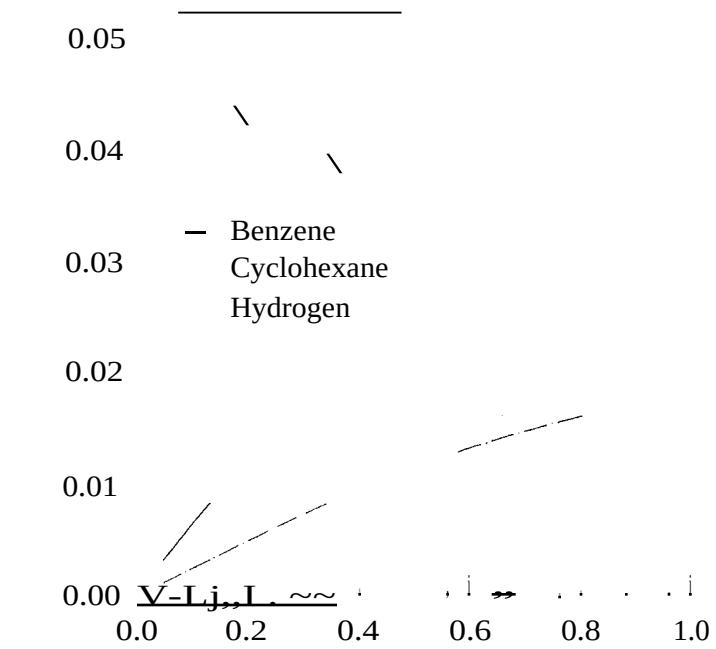

(a)

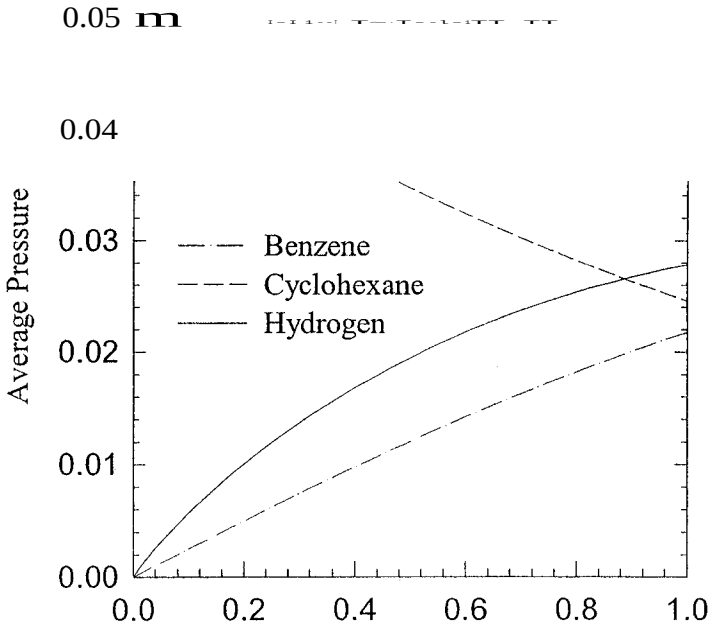

(b)

Figure 15(a,b). Pressure profile of reactive components. (a) Re_p = 2.28; Sweep = 1.0E-04 mol/s; and (b) Re_p = 2.28; Sweep = 1.0E-03 mol/s.

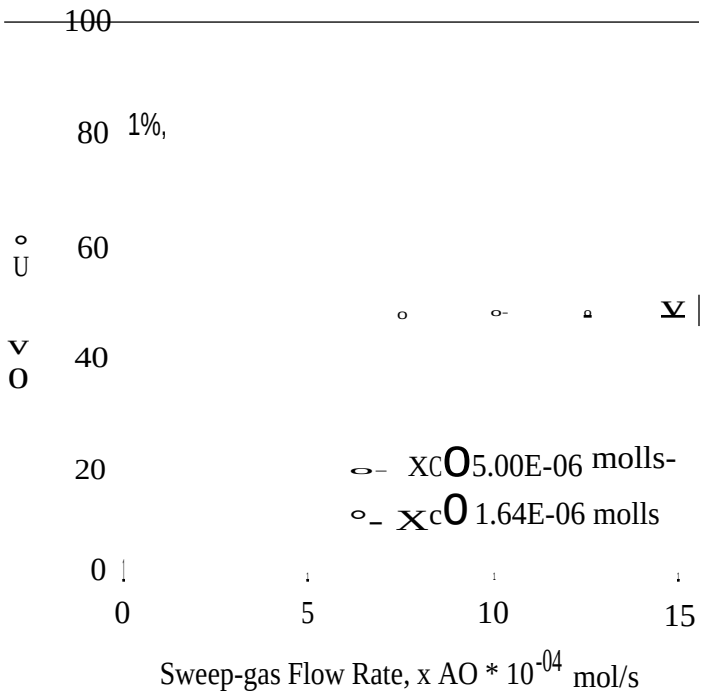

Figure 16. Effect of sweep-gas flow rate on conversion.

THE DEHYDROGENATION OF CYCLOHEXANE IN A PALLADIUM-CERAMIC MEMBRANE REACTOR

The major focus of this research was to investigate the potential application of our electroless deposited Pd-ceramic composite membrane in membrane-reactor configuration for equilibrium limited dehydrogenation reactions. In particular, dehydrogenation of cyclohexane was chosen as a candidate reaction for this study for two reasons. First, it is a low temperature reaction (around 200 °C), and secondly, it has been studied thoroughly in conventional reactors and in some novel membrane reactors by a number of investigators. Itoh [16] used a palladium membrane reactor packed with a platinum catalyst supported on alumina to study the dehydrogenation of cyclohexane by equilibrium shift. Sun and Khang [6] employed a Vycor glass membrane impregnated with platinum while Okubo [22] studied a hollow fiber ceramic membrane reactor packed with Pt/A1203 (3% (w/w)) catalysts to study the same reaction. In this work, we used our Pd-ceramic membrane on planar microporous a-alumina substrate in a packed-bed reactor for dehydrogenation of cyclohexane by equilibrium shift.

PERM-SELECTIVITY STUDY OF CANDIDATE MEMBRANES

As mentioned earlier, we had difficulty in fabricating Pd-stainless steel membrane by conventional electroless deposition process. The Pd-membrane film deformed when exposed to hydrogen environment. With modified electroless deposition, we hope to further improve the Pd film characteristics. For this research, to test membrane reactor-separator concept we examined our Pd-ceramic membrane along with a commercially available hydrogen selective ceramic membrane from Velterop. In this section we discuss their hydrogen permeability characteristics. The membranes tested permeability were in planar disc geometry.

DIFFUSION CELL

Before carrying out dehydrogenation reaction, the permeability tests of the two discs were conducted. Both the permeability tests and the reaction were carried out in a diffusion cell designed by Velterop, model LTC Type K-500. The cell consisted of outer parts, inner parts, graphite seals, Cu seals and the membrane is mounted on non-porous end seal, as shown in Figure 17. The outer parts are made of SS AIS1310 and the inner parts are made of titanium.

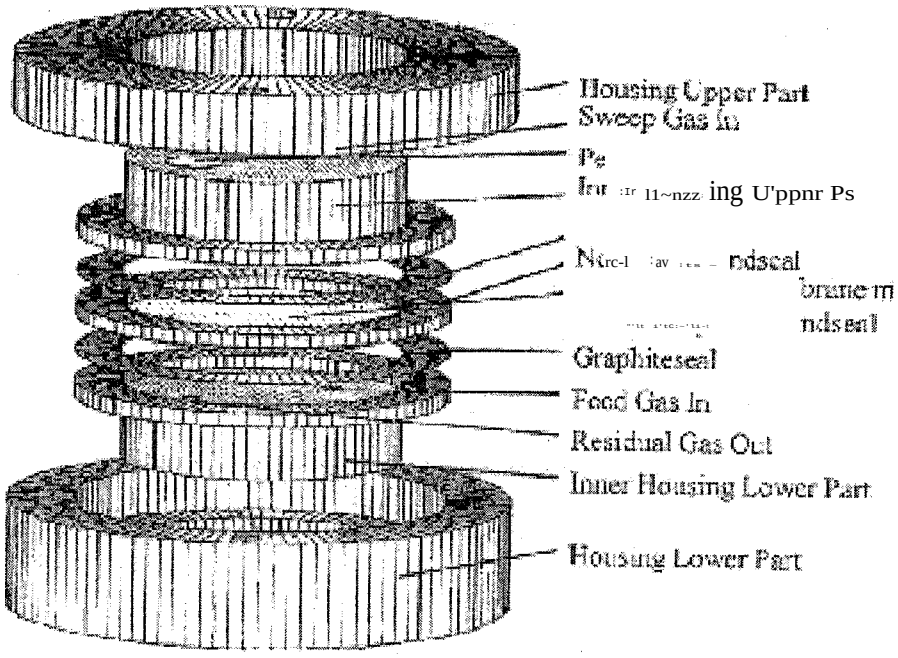

Figure 17. The structure of the diffusion cell

The cell can be heated up to 500 °C. The thermal expansion of the two materials and dimensions are such that at elevated temperature, the inner and outer parts become self-sealing. Graphite seals were used for sealing the ceramic edge and the Cu seals were used for connecting tubes.

MEASUREMENT SETUP

The permeability measurement setup consisted of gas sources, diffusion cell, a tubular furnace, mass flow controllers and a gas chromatograph. The only difference of the reaction measurement is the evaporator of cyclohexane was added in the system (as shown in Figure 18). The membranes were held in between the cell. The cell was mounted and placed in a tubular furnace (Lindberg Type 55347), while both sides of the cell were connected to gas supply lines. All the inlet and outlet gas supply lines were constructed of 1/4 and 3/8 stainless steel tubing. A temperature controller controlled the temperature. Mass flow controllers were used to measure the flow rates of the streams coming in and out of the cell.

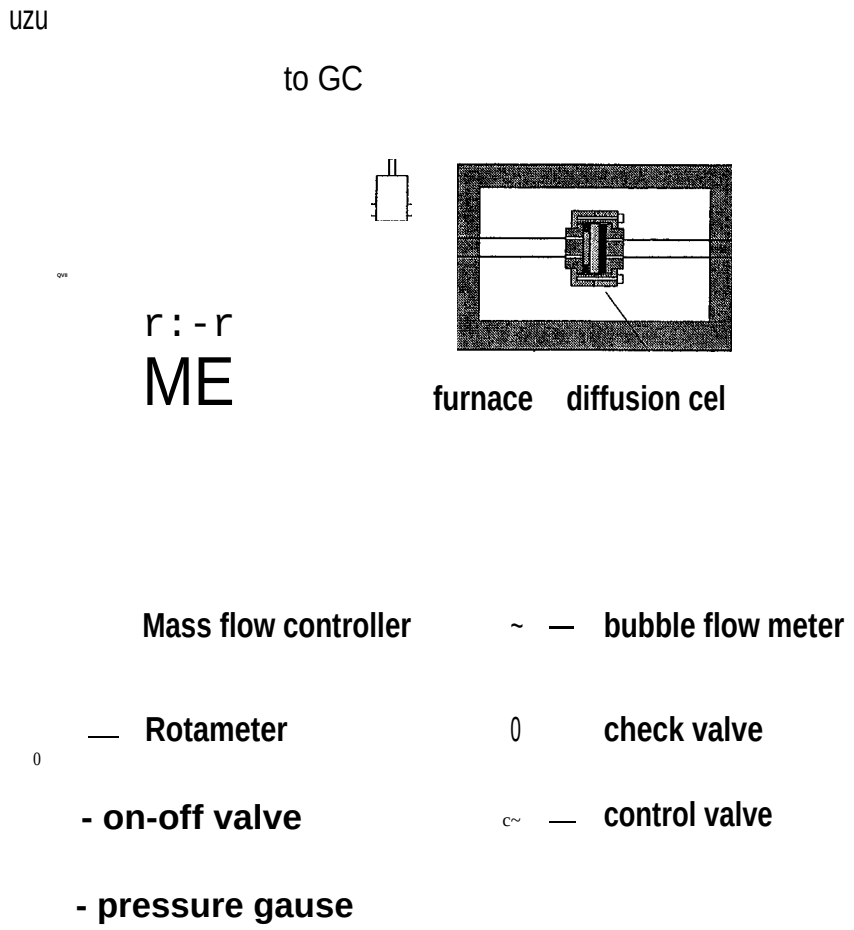

Figure 18. Dehydrogenation of cyclohexane reaction setup

PERMEABILITY TESTS

When diffusion through the bulk metal is the rate-limiting step and hydrogen atoms form an ideal solution in the metal (Sievert's law of hydrogen solubility dependence), n is equal to 0.5. However, values of n greater than 0.5 may result when surface processes influence the permeation rate or when Sievert's law is not followed. To evaluate n, the simplification was made over Eqn. (10) by letting $(PHZ)_{,} << (PHZ)_{HZ}$ and this term was neglected from the right hand of the equation. A plot of log (N^{HZ}) against log $(P^{HZ})_{H,}$ yields a straight line with slope n and from the intercept, the permeability coefficient can be obtained.

The permeability experiments were conducted at temperatures of 373K and 473K. The pressure on the high-pressure side ranged from 10 psig to 20 psig, with an increment of 2.5 psig. The low-pressure side was maintained at 5 psig. The flow rate of the feed and the carrier gas at the permeation side were kept constant for easy comparison.

When the system was connected to the open gas cylinders, the pressure at the high-pressure side must be put on first. Because both membranes were mounted on non-porous ceramic, the structures of the discs were so that the side that was not plated with membrane can stand very little net pressure. If the pressure at the permeate side was put on first, the membranes may tear off from the mount, making it unusable.

After placing the membrane in the diffusion cell, a leak test was performed to detect any leaks in the system. Following the test, the gases were supplied to the system. During startup, the Pd-membrane was heated to 723K under argon atmosphere to avoid hydrogen embrittlement and possible pinhole formation in the palladium film due to heating in a hydrogen atmosphere at temperatures below the critical temperature of the palladium-hydrogen system (about 573K). The system remained untouched for about an hour to reach the steady state. Each gas sample was collected 500 pl from both sides of the system by 1-ml syringe. The collected samples were then injected in the HP6890 Plus Gas Chromatograph for analysis.

To estimate the power of n in Eqn. (10), hydrogen fluxes at various operating temperatures and pressures were plotted on a log-log scale against the partial pressure of hydrogen at the high-pressure side. The plots are shown in Figures 19 and 20 for palladium membrane and hydrogen selective ceramic membrane respectively. For the palladium membrane, the n was 0.51 at 373K and 0.45 at 473K. For the ceramic membrane, the n was 0.50 at 373K and 0.48 at 473K. The comparisons of the power index of palladium membrane and hydrogen selective membrane are shown in Figures 21 and 22 at 373K and 473K, respectively. From Figure 19, we can see the hydrogen flux of the palladium membrane increases with increasing temperature, while the hydrogen flux of the ceramic membrane (Figure 20) is almost temperature ¡ndependent. Although the magnitude of the hydrogen flux of the ceramic membrane is higher than the palladium membrane, it proves that the ceramic membrane is porous.

In earlier work, Fan [9] showed that the selectivity of the Pd-ceramic membrane is significantly higher than Velterop's ceramic membranes. Thus, one would expect higher flux in the ceramic membrane not because of high perm-selectivity, but due to high permeability

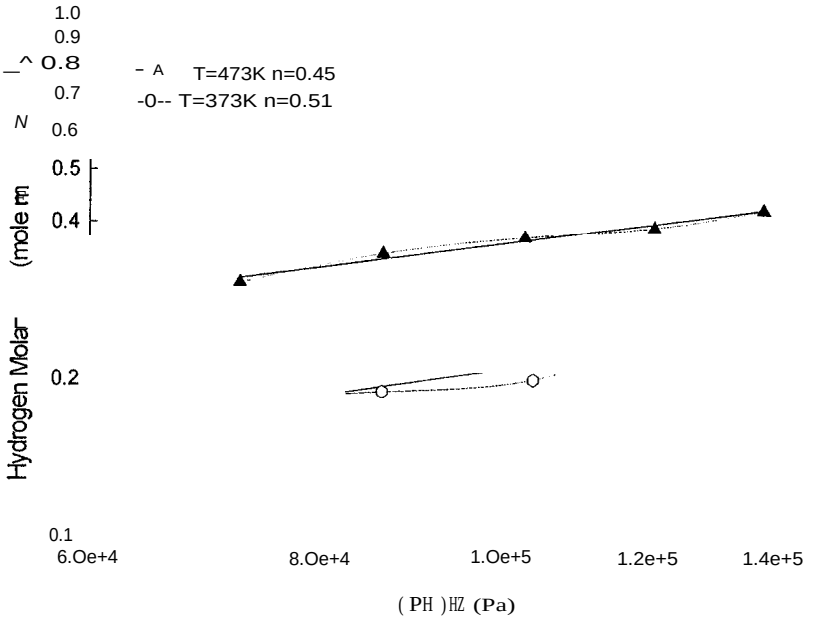

Figure 19. Evaluation of n for the palladium membrane

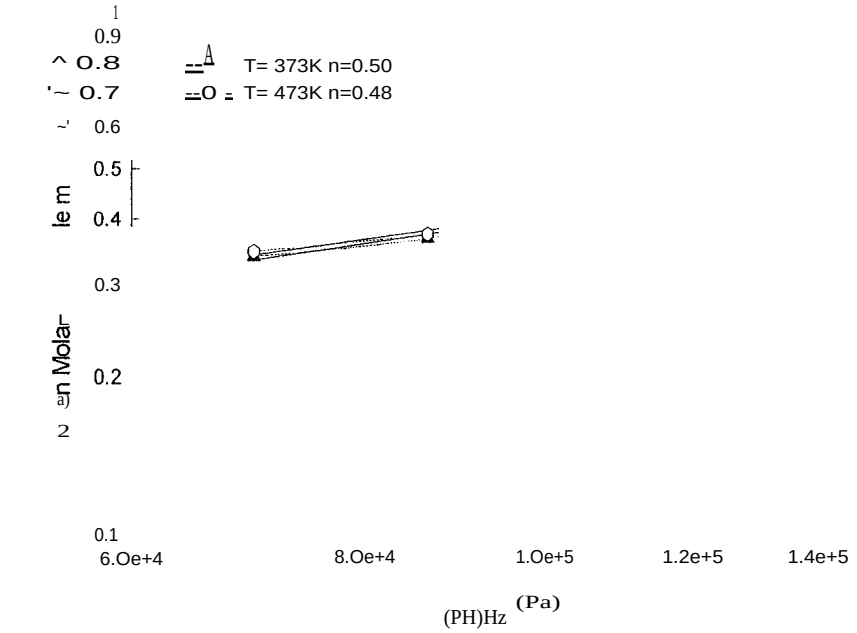

Figure 20. Evaluation of n for HZ selective ceramic membrane

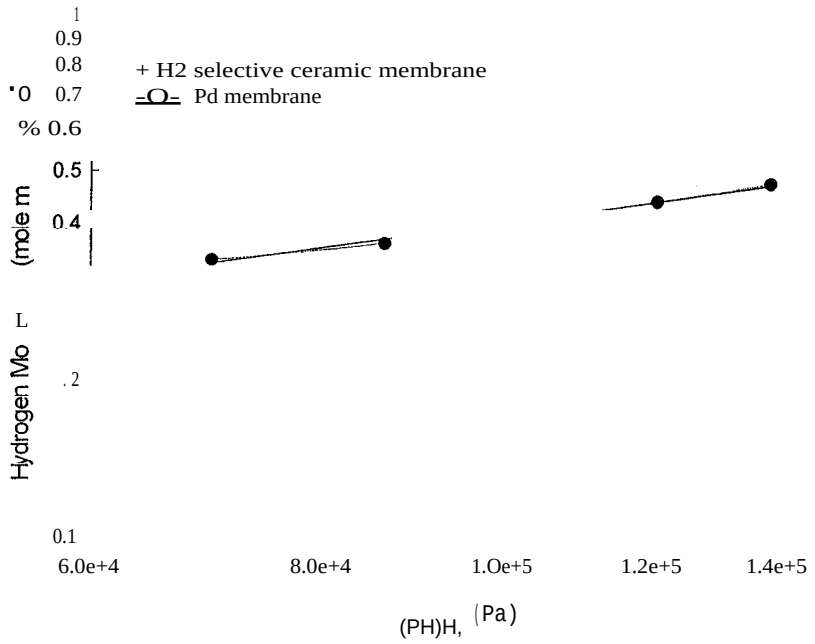

Figure 21. Comparison of hydrogen flux of H2 selective ceramic membrane and Pd membrane at T = 373K

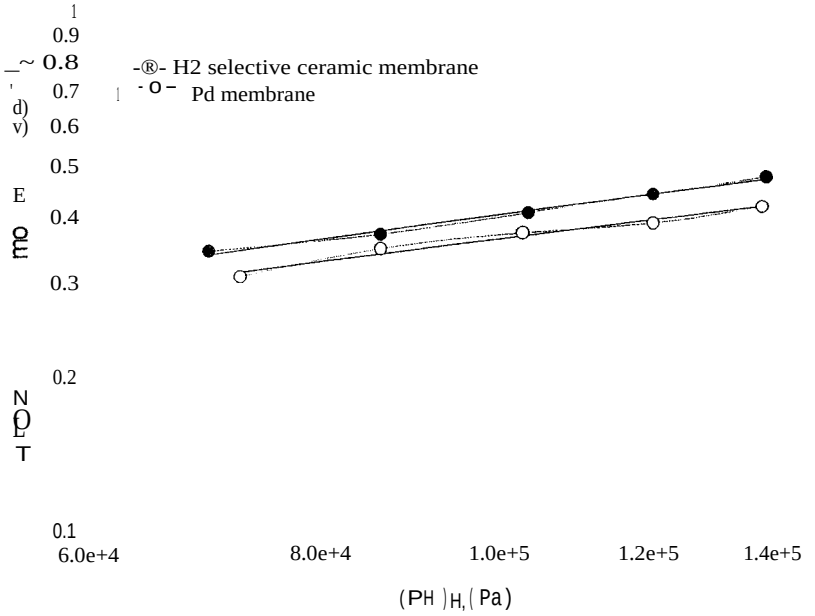

Figure 22. Comparison of hydrogen flux of H2 selective ceramic membrane and Pd membrane at T = 473K

associated with leaky membrane. More evidence would be shown when the reaction of the dehydrogenation of cyclohexane was conducted, there were large amount of cyclohexane and benzene detected at the permeate side.

The hydrogen fluxes plotted against driving force ~ $(P_{H,)x_2} - (P_{Hz})_{AC}$, for Pd membrane are shown in Figures 23 and 24. At a given temperature, the slope of the line provides the value of Q_H/t. Since the membrane thickness is known (about 12pm as determined by weight-gain method), one may calculate the membrane permeability from the known slopes of the lines at various temperatures as shown in Figure 23 and 24. The results of the calculation are tabulated in Table 6.

Table 6. Hydrogen permeability coefficient (mol - m - m-2,. s-1 · Pa")

Temperature (K)	Pd film thickness (12p.m)
373	2.4 x 10_^{S}
473	8.34 x 10-'

DEHYDROGENATION OF CYCLOHEXANE IN MEMBRANE REACTOR

The dehydrogenation of cyclohexane was conducted under atmosphere pressure at 200 °C. About 4 gram of 0.5 wt% Pt/A1$_2$O$_3$ catalysts from Alfa were put in the side faced the palladium membrane. Each time, new catalysts were used for different disks. Ar/C6H12 mixture with 15.7 molar percentage of C6H12 was fed in the cell. The Ar/C6H12 feed ratio was chosen based on modeling work of Mondal [23].

The schematic diagram of the experimental membrane-reactor system is shown in Figure 18. The evaporator of cyclohexane was put on the hot plate, a thermocouple was used to monitor the temperature of the plate. The tube introducing argon into the evaporator was long enough to be beneath the liquid level of the cyclohexane. This helps to make argon well mixed with cyclohexane to get saturated vapor. A check valve, making sure the flow is uni-directional, controlled the stream. The flow rate of the mixture was measured by a bubble flow meter (in this case, the mass flow controller and the rotameter are not appropriate to measure the flow rate,

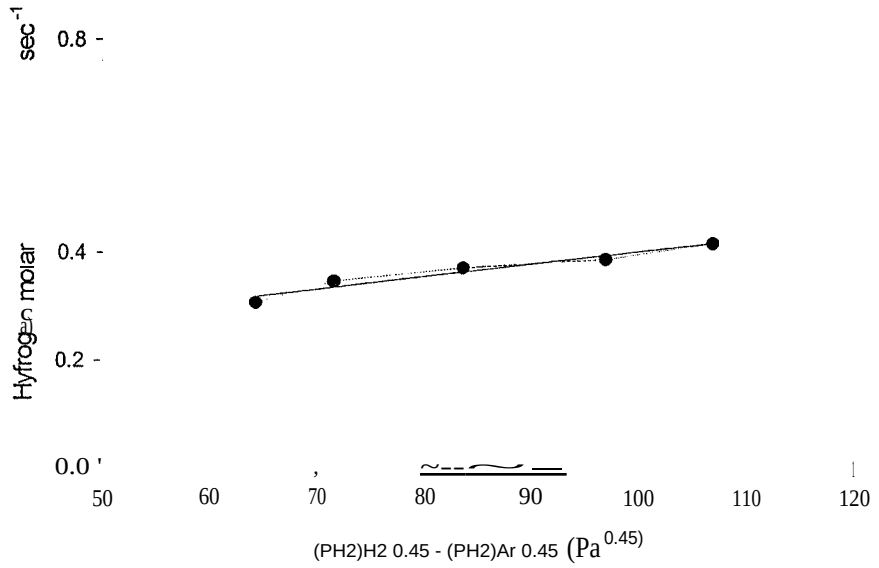

Figure 23. Effects of transmembrane hydrogen partial pressure Difference on flux at T = 373K through Pd membrane

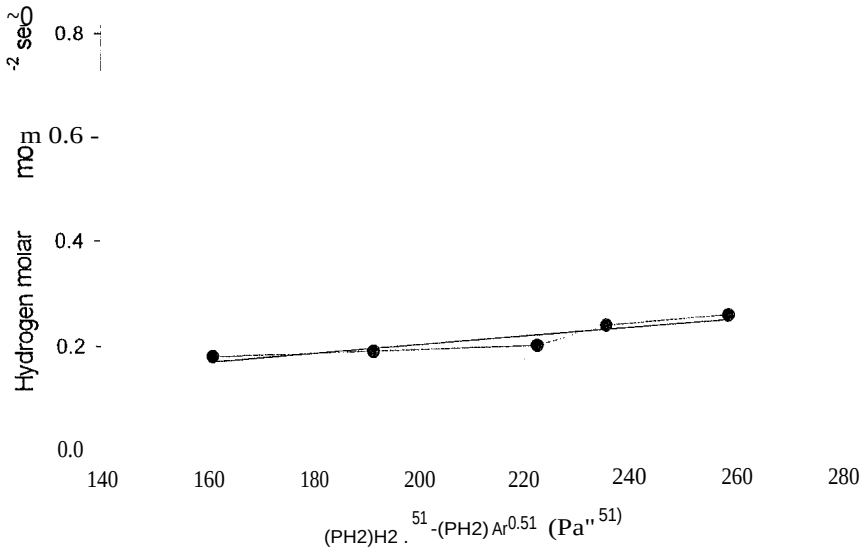

Figure 24. Effects of transmembrane hydrogen partial pressure Difference on flux at T = 473K through Pd membrane

because liquid essence of the vapor is not good for mass flow controller and it is difficult to calibrate rotameter for mixture). Argon was used as the sweep gas at the permeate side to carry hydrogen out.

Different flow rates of feed and different flow rates of sweep gas were set to see the influences of the feed and sweep gas flow rates on the conversion of the reaction. About 0.9×10^{-6} mol / s and 1.37×10^{-6} mol / s were set as the flow rates for cyclohexane. The flow rates of sweep gas were 0, 0.02, 0.05, 0.08, and 0.10 SLPM.

For each sweep gas flow rate, the system was untouched about one hour before samples were taken from the reaction side to determine the conversion of the reaction. The samples at permeate side were taken to see if benzene and cyclohexane also diffused through the membrane. The results are shown in Figures 25 and 26 for the palladium membrane and ceramic membrane, respectively. The dashed lines in the figures show the conventional equilibrium conversion of the reaction at 200 °C, which is about 18.7%. In Figure 25, the highest conversion can reach 56%, which is almost three times of the conventional equilibrium conversion. We also observed, at given sweep gas flow rate, the conversion of cyclohexane to benzene decreases with increasing feed flow rate. It is because the higher the flow rates the lower the resident time of the feed in the system. Also, the influence of the sweep gas indicates that the higher the flow rate of the sweep gases the higher the conversion. The conversion is improved by removing hydrogen away, and the reversible reaction moves to the direction in favor of producing more products. When the sweep gas reach above 0.08 SPLM, the conversion had almost become constant around the flow range of feed used in this project, which means the rate that argon carried hydrogen away is equal to the rate of hydrogen diffusing through the membrane, it is the maximum conversion that sweep gas can help to get, higher flow rate would be no more help for the conversion.

The comparisons of the conversions of two membranes are shown in Figures 27 and 28 for cyclohexane feed flow rates of 1.37×10^{-6} mol / s and 0.9×10^{-6} mol / s , respectively. The palladium membrane can get higher conversion than the ceramic membrane under the same condition. It proves that the palladium membrane is a better candidate to improve the conversion of reversible reactions. The GC results from the permeate side also showed that also 30% of cyclohexane and benzene diffused through the ceramic membrane while there is only trace amount of cyclohexane and benzene detected at the permeate side for the palladium membrane.

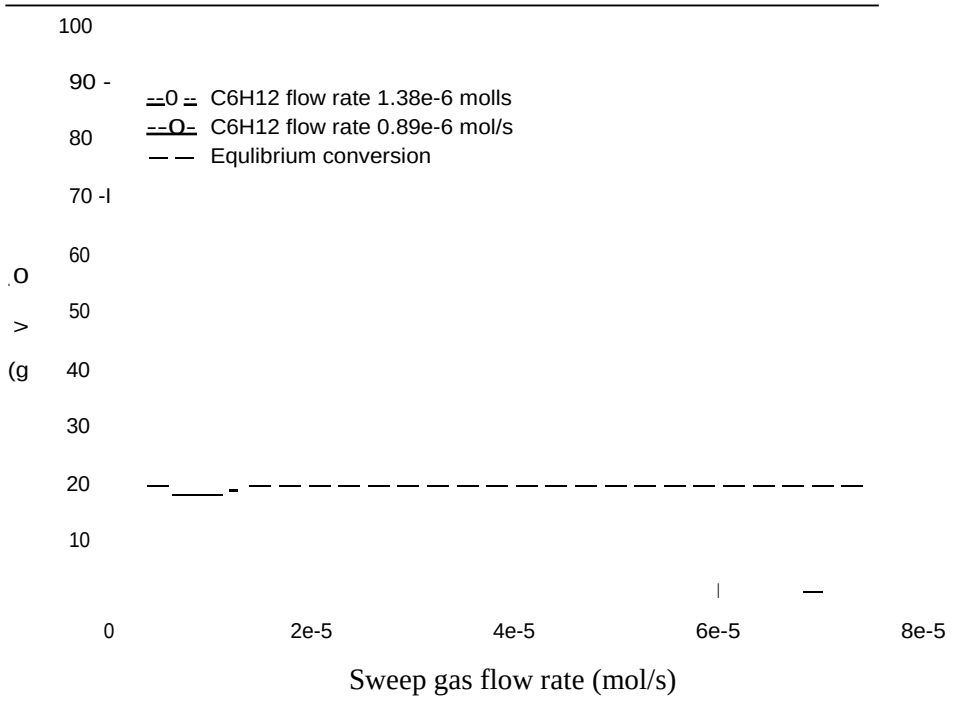

Figure 25. Sweep gas influence to the conversion of palladium membrane disk

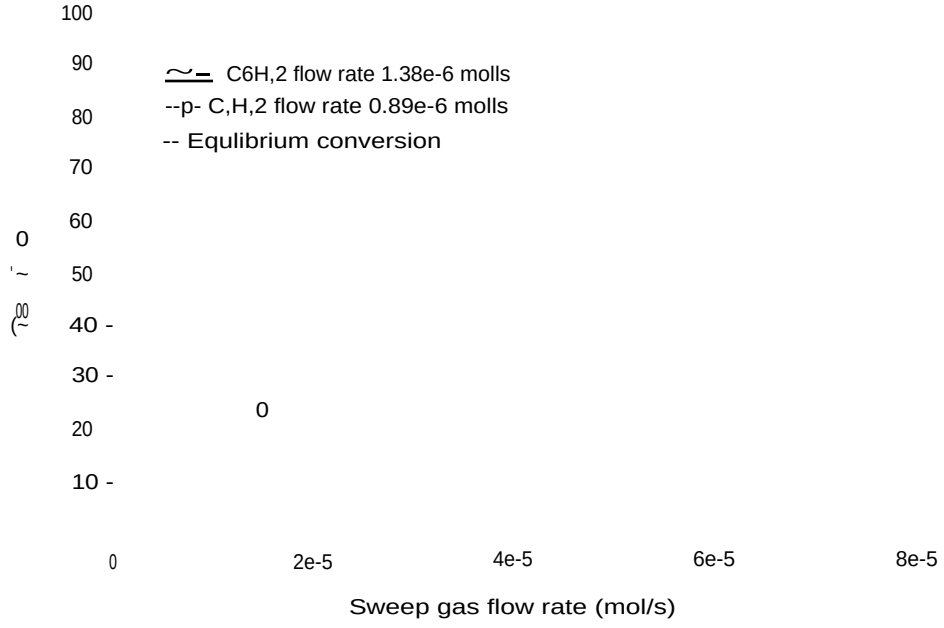

Figure 26. Sweep gas influence to the conversion of the H2 selective ceramic membrane disk

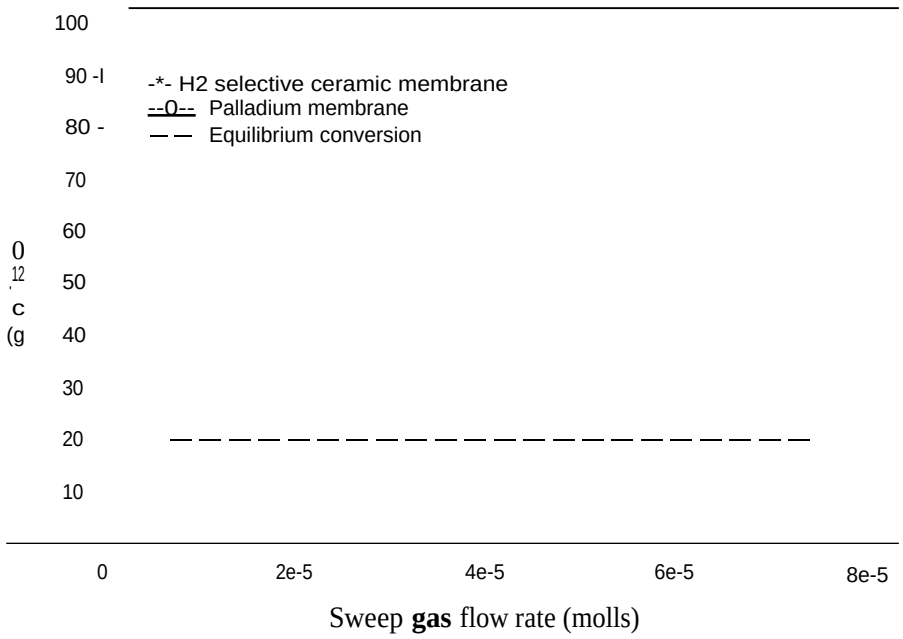

Figure 27. Conversion comparison of H2 selective membrane and Palladium membrane at flow rate 1.37x 10-6 mol / s

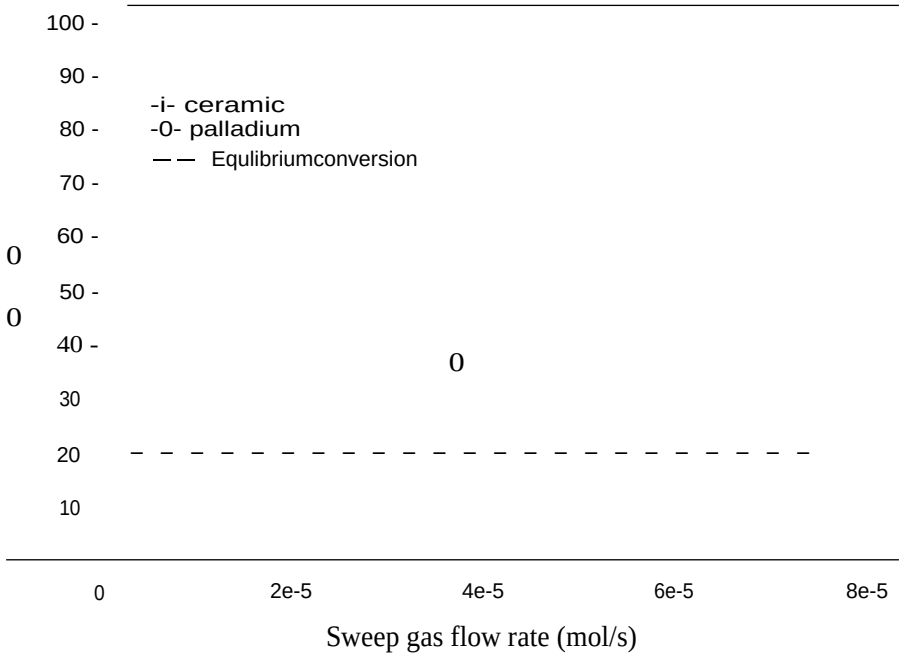

Figure 28. Conversion comparison of HZ selective membrane and Pd membrane at flow rate 0.89x10-6 mol/s

The comparisons of GC outputs at reaction side and permeate side for the two membranes are given in Figures 29 and 30, respectively.

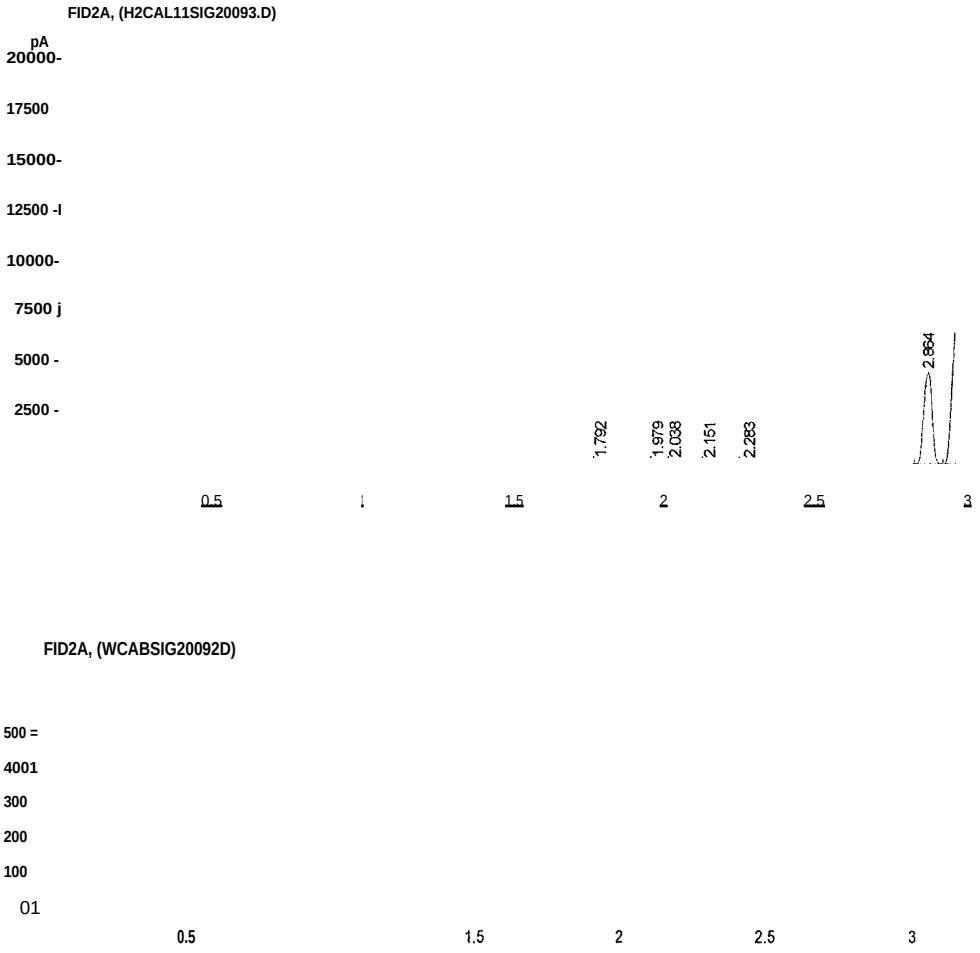

Figure 29. GC results from (a) reaction side (b) permeate side of the Pd membrane. Both the ratios of Benzene and cyclohexne in (a) and (b) are 45:1

When the palladium membrane was taken out from the cell, the areas which directly faced the tubing ends where gas came in and out of the system were darker than the other places. The SEM and EDX results of this area are shown in Figures 31 and 32, respectively. From the SEM result, there are some micro-cracks in the palladium film and the EDX result showed more Al content than before reaction. We think there is some shrinkage of the palladium membrane at those areas because of the direct flow influence.

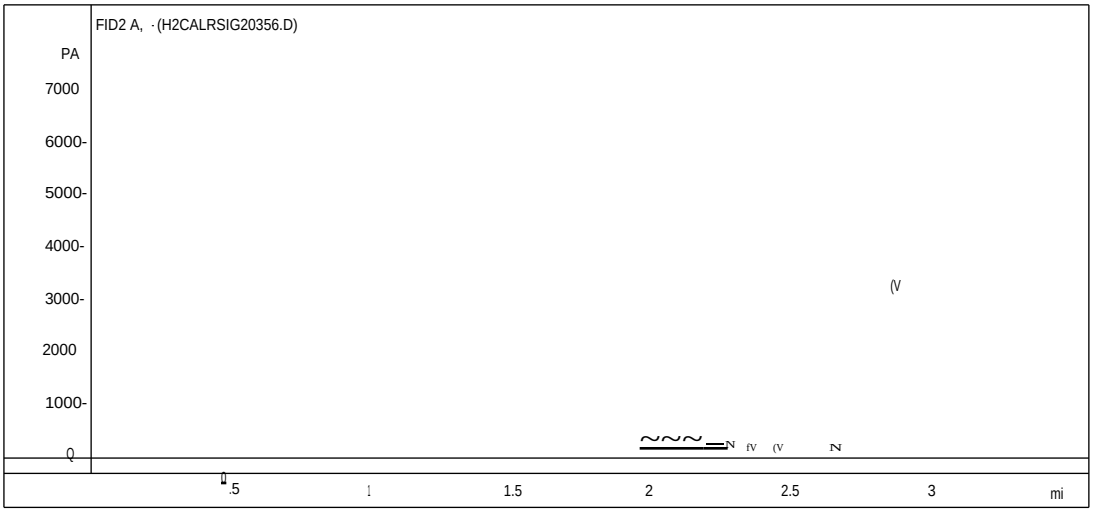

(a)

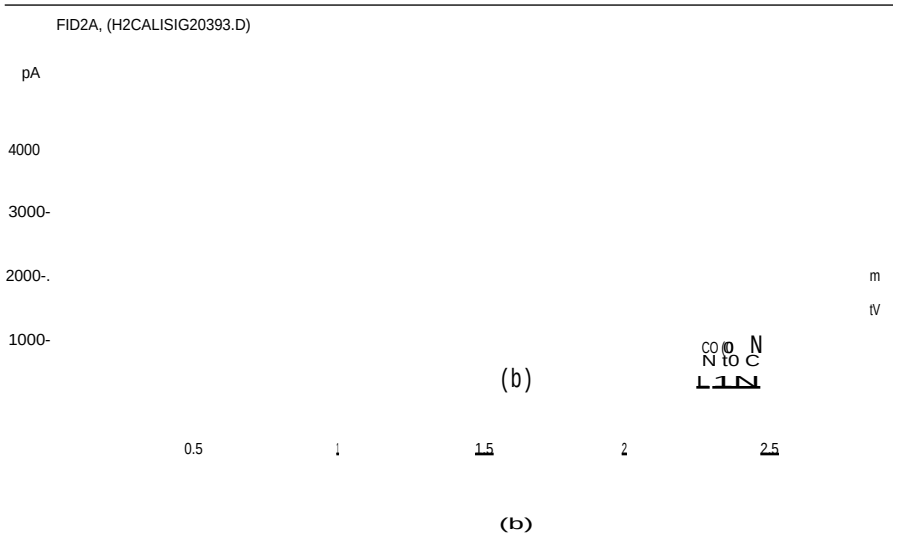

(b)

Figure 30 GC results from (a) reaction side (b) permeate side of the H2 selective ceramic membrane. The ratio of Benzene in (a) and (b) is 3:1. The ratio of Cyclohexane is 7:3.

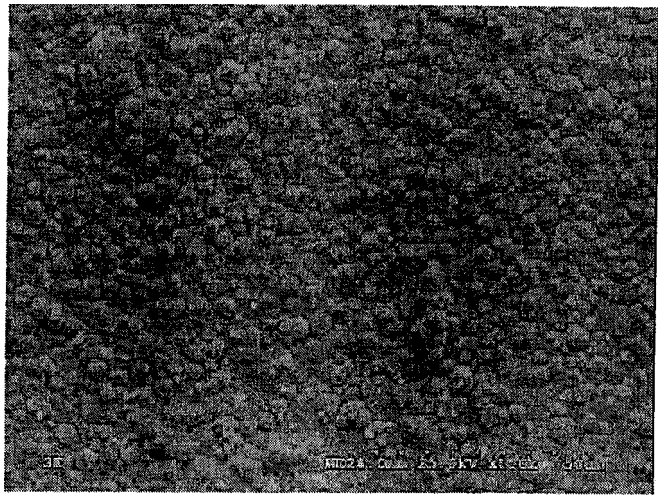

Figure 31. SEM of the area after reaction

Spect. Type	Element	Atomic
ED	7.61	23.45
ED	1.93	5.72
ED	0.22*	0.29*
ED	90.24	70.55
	100.00	100.00

Figure 32. EDX result of the area after reaction

CONCLUSIONS

The electroless plating of eight different kinds of substrates indicates that the structure of the substrate is the fundamental factor to influence the structure of the palladium membrane plated on the substrate. The pore size and coarseness of the substrate are the most important factors when choosing the right substrate for good Pd membrane plating. A modified electroless plating procedure had was developed to plate a better membrane on stainless steel substrate than the conventional method. The reaction of dehydrogenation of cyclohexane had been carried out in diffusion cell. With the help of the Pd membrane, the reaction can reach Super-equilibrium State. For conventional conversion of 18.7% at 200 °C, a conversion of 56% can be reached in palladium membrane reactor by selective removal of hydrogen. To attain favorable equilibrium shift for reversible reactions, the Pd membrane made by this project is a better choice than the hydrogen selective membrane available from Velterop.

ACKNOWLEDGMENTS

This research was sponsored by the Pittsburgh Energy Technology Center, U.S. DOE under grant number DE-FG22-96PC96222. The authors wish to thank their industrial collaborator, Amoco Chemical Company - R&D Center, Naperville. In particular, the support of Dr. Carl Udovich is greatly appreciated. The project also supported (fully/partially) following graduate students in completing their M.Sc. ChE degrees:

Mondal, A.M., "Stability in Single-Stage gas Permeation and Dehydrogenation of cyclohexane in Pd-Ceramic Membrane Reactor," M. S. Thesis, North Carolina A&T State University, 1998.

Chen, Y., "Dehydrogenation of Cyclohexane by Equilibrium Shift in a Palladium-Ceramic Membrane Reactor," M. S. Thesis, North Carolina A&T State University, 2000.

REFERENCES

1. Shu, J., Grandjean, B.P.A., "Catalytic palladium-based membranes reactors: a review," Can. J. Chem. Eng, 69,1036 (1991).

2. Armor, IN., "Catalysis with permselective inorganic membranes," Applied Catalysis, 49, 1 (1989).

3. Wu, J.C.S., Gerdes,T.E., Pszczolkowski, J.L., Bhave,R.R., and Liu, P.K.T., "Dehydrogenation ethylbenzene to styrene using commercial ceramic membranes as reactors," Sep. Sci. Technol, 25, 1489 (1990).

4. Ziaka,Z.D, Minet R.G., and Tsotsis,T.T., "Propane dehydrogenation in a packed-bed membrane reactor," AIChE J., 39, 526 (1993).

5. Champagnie, A.M., Tsostsis,T.T, Minet,R.G, and Webster,I.A., "A high temperature membrane reactor for ethane dehydrogenation," Chem. Eng. Sci., 45, 2423 (1990).

6. Sun Y.M., Khang.S.J., "Catalytic membranes for simultaneous chemical reaction and separation applied to dehydrogenation reaction," Ind. Eng. Chem. Res., 27, 1136 (1988).

7. Bhave, R.R., Inorganic Membranes: Synthesis, Characteristics and Applications, New York: Van Nostrand Reinhold, 1991.

8. Su, N., Preparation and Characterization of Palladium-Ceramic Composite Membrane for High Temperature Gas Separation. M.S. Thesis, North Carolina A&T State University, 1995.

9. Fan, T., Perm-selectivity of Hydrogen Through Electroless Deposited Thin-film Palladium-Ceramic Composite Membrane. M.S. Thesis, North Carolina A&T State University, 1996.

10. Yeung, K.L., Christiansen, S.C., "Palladium composite membranes by electroless plating technique: Relationships between plating kinetics, film microstructure and membrane performance," J. Memb. Sci., 159, 107 (1999).

11. Yeung, K.L., Aravind, R., "Metal composite membranes: synthesis, characterization and reaction studies," Studies in Surface Science and Catalysis, 101, 1349 (1996).

12. Glasstone, S., Physical Chemistry, Van Nostrand, 1946

13. Denbigh, K. G., Principles of Chemical Equilibrium, Cambridge University Press, 1981

14. Shinji, O., Misono, M., and Yoneda, Y., "The Dehydrogenation of Cyclohexane by the Use of a Porous-Glass Reactor," Bull. Chem. Soc. Japan, 55, 2760 (1982).

15. Itoh, N., Tanabe, H., Shindo, Y., and Hakuta, T., "Kinetic Analysis of Cyclohexane Dehydrogenation over Platinum Catalyst," Sekiyu Gakkaishi, 28,323 (1985b).

16. Itoh, N., "A Membrane Reactor Using Palladium," AIChE. J., 33,1576 (1987).

17. Hulbert, R. C. and Konecny, J. O., "Diffusion of Hydrogen through Palladium," J. Chem. Phys., 34,655 (1961).

18. Sieverts, A., and Danz, W., "Solubility of D2 and H2 in Palladium," Z. Physik. Chem., 34(B), 158 (1936).

19. Collins, J. P. and Way, J. D., " Preparation and Characterization of a Composite Palladium-Ceramic Membrane," Ind. Eng. Chem. Res., 32,3006 (1993).

20. Ilias, S., Su, N., Udo-Aka, U. I., and King, F. G., "Application of Electroless Deposited Thin-Film Palladium Composite Membrane in Hydrogen Separation," Sep. Sci. Technol., 32, 487 (1997).

21. Wen, C. Y., and Fan, L. T., Models for Flow Systems and Chemical Reactors, Dekker, New York, 1975.

22. Okubo, T., Haruta, K., Kusakabe, K, Morooka, S., "Equilibrium shift at short space-time with hollow fiber ceramic membrane," Ind. Eng. Chem. Res., 30, 614 (1991).

23. Mondal, A.M., "Stability in Single-Stage gas Permeation and Dehydrogenation of cyclohexane in Pd-Ceramic Membrane Reactor," M. S. Thesis, North Carolina A&T State University, 1998.